Probability Cost-Benefit Analysis for Ship Structural Design

Tiago Brazinha Pereira

Thesis to obtain the Master of Science Degree in

Naval Architecture and Ocean Engineering

Supervisor: Doutor Yordan Ivanov Garbatov

Examination Committee

Chairperson: Doutor Ângelo Manuel Palos Teixeira

Supervisor: Doutor Yordan Ivanov Garbatov

Member: Doutor Manuel Filipe Simões Franco Ventura

July 2022

DECLARATION

I declare that this document is an original work of my authorship and fulfils all the requirements of the Code of Conduct and Good Practices of the Universidade de Lisboa.

Signature

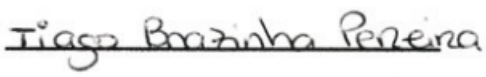

ACKNOWLEDGEMENTS

First, I want to express my deep gratitude to my advisor and professor, Dr Yordan Garbatov, for his guidance, availability, motivation, knowledge and help in completing this study, for your corrections and opinions in the direction of constant improvement throughout my dissertation.

To my family, especially my parents, Manuela and João, my grandparents, Manuela and José, and my brother Diogo, for the immense patience, motivation, understanding and all support throughout my academic study and in the accomplishment of the thesis.

To my friends and colleagues, of course, for patience, help, knowledge and friendship in overcoming various obstacles throughout my academic career.

To the ONE OCEAN project company, especially to Eng. José Cruz and my colleague engineers Lidia Correia and Miguel Leal for the help and availability in the realisation of the dissertation.

RESUMO

O objetivo da presente dissertação é dimensionar e otimizar a secção mestra de um navio polivalente baseado na análise probabilistica de custo benefício.

É dimensionado a secção mestra típica para este tipo de navio, cumprindo os requisitos mínimos impostos pela Sociedade Classificadora (SC), Bureau Veritas (BV, 2019). A partir do dimensionamento realizado obtêm-se as espessuras mínimas das chapas, a área de corte e o módulo de secção mínimo, cumprindo com os carregamentos impostos pela SC, encurvadura das chapas e perfis e resistência última. O software *MARS2000* disponível gratuitamente no sítio da Sociedade Classificadora (SC) Bureau Veritas (BV, 2019), e o software *MS EXCEL* são utilizados como recursos no dimensionamento da secção mestra.

O método de fiabilidade de primeira ordem (FORM) é aplicado para identificar, avaliar e analisar o comportamento de risco da estrutura na redução da probabilidade de falha, Estado Limite Último (ULS), em relação ao colapso progressivo.

A estimativa de custos iniciais do investimento de construção associado aos custos dos materiais utilizados, fabrico e mão-de-obra, para este tipo de navio é estimado através do CAPEX (*Capital Expenditure*).

A otimização estrutural consiste na minimização do custo de construção a uma fiabilidade de alvo predefinida. O comportamento de risco associado ao nível de fiabilidade da estrutura irá também ser analisado em relação ao impacto a questões económicas, como a flutuação dos preços de matérias-primas.

Palavras-Chave: Dimensionamento; Índice de Fiabilidade; Probabilidade de Falha; Estimativa de Custos (CAPEX); Análise Probabilistica de Custo Benefício; Otimização.

ABSTRACT

The objective of the present thesis is to design and optimise the midship section of a multi-purpose ship based on a probability cost-benefit analysis.

The midship section is designed to comply with the minimum requirements imposed by Classification Society Rules (CS), Bureau Veritas (BV, 2019). The minimum thickness of the plates, the shear area and the minimum hull section modulus are obtained from the dimensioned performed, complying with the design loads imposed by the CS, buckling of the plates and profiles and ultimate strength. The *MARS2000* software is available free of charge on the website of the Classification Society (CS) Bureau Veritas (BV, 2019), and the *MS EXCEL* software are used as a resource in the design of the midship section.

The first-order reliability method (FORM) is employed to identify, assess and analyse the risk behaviour of the structure in reducing the probability of failure, Ultimate Limit State (ULS), about progressive collapse.

The estimate of the initial costs of the construction investment associated with the costs of materials used, manufacturing and labour of this type of ship is estimated through CAPEX (Capital Expenditure).

Structural optimisation consists of minimizing the construction cost and predefined target reliability. The risk behaviour associated with the reliability level of the structure will be analysed concerning the impact of economic issues, such as the fluctuation of raw materials prices.

Keywords: Design; Reliability Index; Probability of Failure; CAPEX estimation; Cost-Benefit Analysis; Optimisation.

TABLE OF CONTENTS

LIST OF FIGURES

LIST OF TABLES

LIST OF ACRONYMS

ABS – American Bureau Shipping;

ALS – Accidental Limit State;

BV – Bureau Veritas;

CAPEX – Capital Expenditure;

CATS - Cost of One Ton Accidentally Spilt Fuel Oil;

CCS – China Classification Society;

CDF – Cumulative Distribution Function;

CRS – Croatian Register of Shipping;

CS - Classification Society;

DECEX – Decommissioning Cost;

DMF – Design Modification Factor;

DNV GL – Det Norske Veritas and Germanischer Lloyd;

FLS – Fatigue Limit State;

FORM – First-Order Reliability Method;

GDP – Gross Domestic Product;

HTS – High Tensile Steel;

IACS – International Association of Classification Societies;

ICAF – Implied Cost of Averting the Fatality;

IMO – International Maritime Organization;

IRS – Indian Register of Shipping;

KR – Korean Register of Shipping;

LCC – Life Cycle Cost;

LR – Lloyd's Register;

MARAD – Maritime Administration;

NKK – Nippon Kaiji Kyokai;

OPEX – Operational Cost;

PDF – Probability Density Function;

PRS – Polish Register of Shipping;

RINA – Registro Italiano Navale;

RS – Russian Maritime Register of Shipping;

SFOC – Specific Fuel Oil Consumption;

SLS – Serviceability Limit State;

SOLAS – Safety of Life at Sea;

TEU – Twenty-feet Equivalent Unit;

ULS – Ultimate Limit State;

1. INTRODUCTION

The initial stage of the design of a marine structure or a ship consists of the iterative process of decision making, considering certain aspects that must be considered, such as the type of service, cargo transported, velocity, etc., to determine the ideal structural configuration. One of the main steps of the project is the structural analysis, whose objective is to design and determine an efficient and optimised structure.

Due to the maritime accidents that occurred in the early 19th century, the International Maritime Organization (IMO) developed Rules and regulations that regulated the ship's design to maintain safety in the maritime sector. In 1969, IMO gave responsibility for applying maritime safety Rules and standards to the International Association of Classification Societies (IACS).

IACS members develop and guide the technical support needed to unify interpretations of international legal standards. These interpretations are applied by each member in certifying compliance with legal provisions on behalf of flag states to provide statuary and classification services. Members belonging to IACS are American Bureau Shipping (ABS); Bureau Veritas (BV); China Classification Society (CCS); Det Norske Veritas and Germanischer Lloyd (DNV GL); Korean Register of Shipping (KR); Lloyd's Register (LR); Nippon Kaiji Kyokai (NKK); Registro Italiano Navale (RINA); Russian Maritime Register of Shipping (RS); Croatian Register of Shipping (CRS); Polish Register of Shipping (PRS) and Indian Register of Shipping (IRS).

The classification of the ship following the regulations imposed by the classification societies does not consider the economic viability of the ship.

Due to increased competition in maritime transport, it is necessary to design and optimise more efficient structures with a reasonable level of reliability for a lower construction cost, and consequently lower structural weight, and not only comply with the minimum values required by the standards of classification societies.

1.1 Aim and scope

This thesis aims to design and optimise the midship section of a multipurpose ship based on the probability cost-benefit analysis.

From the Rules of the Classification Society (CS) and the *MARS2000* software, it is possible to determine the minimum thicknesses and section modules of the plates and profiles used in the midship section. Structural strength is determined against buckling and yielding, and ultimate strength calculations include plates and stiffeners. The designer will have to decide which thickness and module of the section to use, according to the minimum requirements.

The first-order reliability method (FORM) is employed to identify, assess and analyse the risk behaviour of the structure when the ship is subjected to several loads. The structural elements are evaluated against failure modes related to the Ultimate Limit State (ULS) in the progressive reduction of the probability of failure about the progressive collapse.

Damyanliev (2001, 2002) and Damyanliev et al. (2017) developed regression equations for estimating vessel weights, recalibrating the equations using data from five recently built multipurpose vessels of similar dimensions.

The parameterised estimate of the initial costs of the construction investment associated with the costs of labour, manufacturing and the materials used is estimated through CAPEX (Damyanliev et al., 2017, Garbatov and Georgiev, 2017, Garbatov et al., 2017). CAPEX (Capital Expenditure) is determined through regression analysis based on project parameters, such as weight, ship dimensions, propulsion power, etc.

The optimisation is performed to find a structural design of a reasonable degree of reliability (reduction of the probability of failure) for the most negligible weight of the structure and, consequently, the lowest cost of construction (CAPEX costs). External factors such as the price of raw materials are implemented in the study of structural design optimisation.

1.2 Work structure

The present thesis is structured in seven chapters that follow: **Chapter 2** introduces state of the art on concepts used; **Chapter 3** presents the midship section to be studied and its design according to the Rules of the classification society; **Chapter 4** introduces the first order reliability method (FORM) used to determinate the risk behaviour of the midship section in reducing the probability of failure with the progressive collapse; **Chapter 5** evaluates the estimated lightweight of the ship and the initial construction costs (CAPEX); **Chapter 6** presents the results obtained from the study of the risk-benefit analysis of midship section optimisation; **Chapter 7** presents the conclusion of this study.

2. STATE OF THE ART

The main objective of the ship's structural design is to generate information needed to build a ship within the requirements of class Rules and customers, which is a complex and interactive process. The ship design goes through a series of evolutionary stages converging to a single point, and the most traditional method is spiral design (Evans, 1959).

The optimisation of a structure or project differs between the initial stages of the project. Looking at the spiral design in *Figure 2.1*, we can identify several stages of the project, usually carried out by different teams:

- Main dimensions.
- Hull form.
- General arrangement.
- Resistance and Propulsion.
- Structure (material, scantling, hull section modulus, etc.).
- Stability and Manoeuvrability.
- Costs.
- Safety (Class Rules, IMO, SOLAS).
- Production.
- Etc.

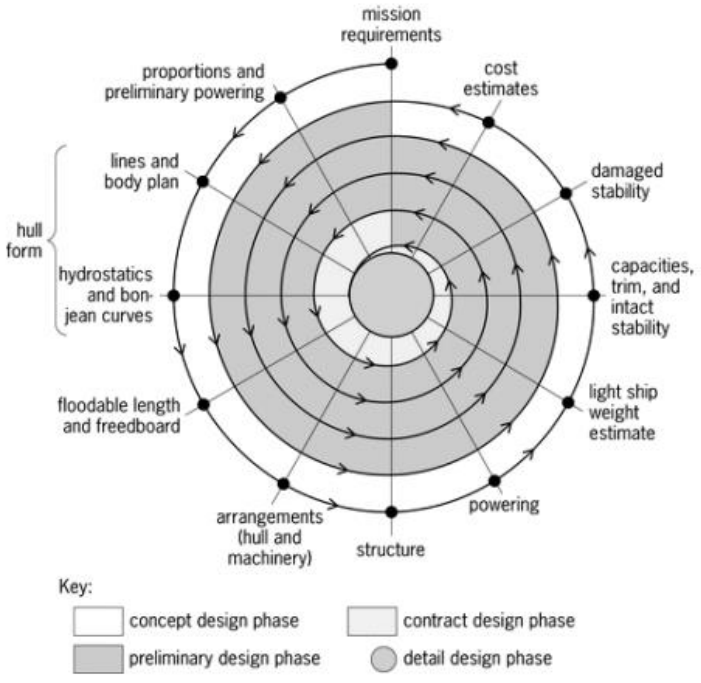

Figure 2.1 – Ship design spiral (Evans, 1959).

So, according to *Figure 2.1*, the main phases of ship design where an assignment of the different tasks are:

- Concept design.
- Preliminary design.
- Contract design.
- Detail design.

The first stage of a ship's design begins with the shipowner's decisions and requirements, always respecting the Rules of classification societies based on current market expectations, thus defining the ship's initial parameters. In the concept design of the ship, the main objective is to achieve the project's feasibility, and in the preliminary design, the objective is its planning. In the contract design, the project's cost is determined. The detailed design aims to carry out the Technical Design, which contains all drawings, documents, and calculations approved by the Classification Society and National Authority.

Ideally, the type of ship to be designed must be passed through all the steps described in the design spiral to obtain a project with a high level of reliability. In the past, the project stages were executed sequentially, but at present most are obtained through an engineering process (Caprace, 2010, Rigo & Caprace, 2011), *Figure 2.2*, increasing efficiency and reducing delivery time.

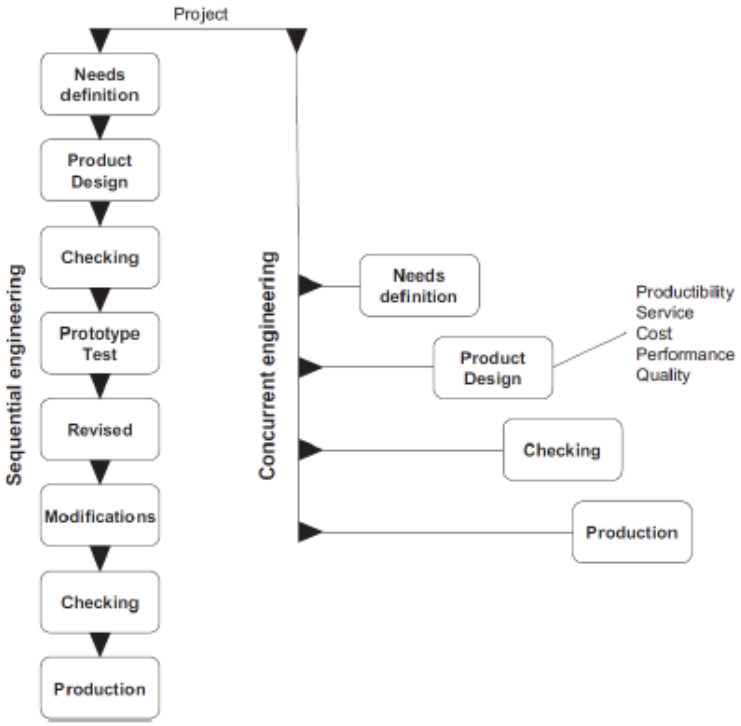

Figure 2.2 – Sequential vs Concurrent Engineering (Caprace, 2010).

As it progresses in the various stages of the project has a higher cost (Ross et al., 2002). *Figure 2.3* shows the decreasing ability to influence the outcome of a project (Caprace, 2010, Rigo & Caprace, 2011). Large groups of designers and shipyards carry out simultaneous design tasks, which is a

common practice. The optimisation of the ship design is one of the many tasks that the naval engineer performs during the various stages of the design spiral (Caprace, (2010), Rigo & Caprace, (2011)).

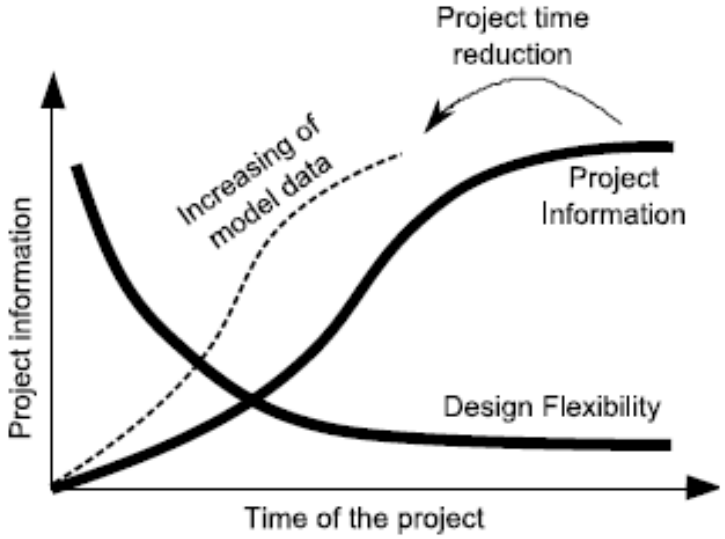

Conceptual Design	Basic Design	Detailed Design
Strategical Decision	Tactical Decision	Operational Decision
2-3 weeks	2-3 months	5-10 months

Figure 2.3 – Design Stage in Shipbuilding Industry (Caprace, 2010).

Each loop of the design spiral can be considered an iteration of the optimisation process, where each step occurs a local optimisation. Local optimisation approaches a specific problem by fixing others, an old industry practice. Using numerical tools specializing in design tasks, it is possible to optimise the shape of the hull to increase speed, reduce fuel consumption and pollutants, optimise the structural design of the ship by reducing its weight or cost of production, etc. (Caprace, 2010, Rigo & Caprace, 2011).

Several studies prove that sequential local optimisation may not lead to global project optimisation, in which tasks are considered simultaneously using the same data and initial design. However, it is currently impossible to achieve a global optimisation with the current technologies available in the naval industry, with the current practice being a local optimisation (Caprace, 2010, Rigo & Caprace, 2011).

Using different optimisation techniques, many researchers have tried to solve the problem of ship design, traditionally a sequential and iterative process, allowing the development of more competitive projects.

Harlander (1960) began the first studies of optimisation of ships and maritime structures, performing calculations by hand. In the following years, Evans et al. (1963) and Nowacki et al. (1970) developed

computer-aided design and optimisation algorithms. Hughes et al. (1980) and Hughes (1988) developed essential steps in optimising structures.

Currently, optimisation tools take a more general approach becoming more reliable, in contrast to what was done in the past.

Seo et al. (2003), Rigo et al. (2003), Khajehpour et al. (2003), Parsons et al. (2004), Klanac et al. (2004) and Cho et al. (2006) developed the techniques of design and optimisation. Later Zanic et al. (2005) and Xuebin (2009) incorporated multicriteria optimisation models that integrate the structural weight and its cost of production.

The structural design of the ship consists of two distinct phases:

- Preliminary Project.
- Detail Design.

The preliminary project determines the position and spacing of ordinary stiffeners and primary supporting members. The detail design determines the geometry, local reinforcement, connections and notches until they reach satisfactory scantling, which fulfils the project criteria.

For the design of any structure, it is necessary to consider the following aspects:

- Define critical failure modes.
- Determine the type of cargo to which the structure will be subjected during its operational life.
- Performing an estimate of weight and centre of gravity when developing a structural configuration.
- Create a simplified model of the structure developed that sufficiently represents the actual model of the structure.
- Compare the structure's performance with various design criteria, for different failure modes that may occur.
- Modify the structural configuration for proper performance and optimisation levels, thus avoiding unnecessary costs.

The ship structural design aims to design the most optimised structure, more efficient with certain factors such as production costs, weight and safety index.

3. DESIGN OF MIDSHIP SECTION OF MULTI-PURPOSE SHIP

3.1 Case study

Multi-purpose ships can carry cargo with different characteristics from other types of ships. They can simultaneously carry various types of cargo: containers, refrigerated cargo, general cargo, bulk cargo, steel products, chemicals, etc.

The present study intends to design the midship section of a multi-purpose ship equipped for carriage containers, with additional service GRABLOADING, i.e., ships with holds tank tops specially reinforced for loading/unloading cargoes using buckets or grabs (BV, 2019), whose main dimensions are in *Table 3.1*.

Table 3.1 – Main dimensions on the vessel considered.

Rule Length, *L* [m]	115.07
Moulded Breadth, *B* [m]	20.00
Depth, *D* [m]	10.40
Moulded Draught, *T* [m]	8.30
Block Coefficient, C_B [-]	0.72
Maximum Service Speed, V_S [knots]	14.00
Deadweight, *DWT* [t]	9 800
Effective Propulsive Power, P_W [kW]	5 400
Number of Crew Members, *NE* [Pax]	20
Number of Superstructure Decks, *NJ* [-]	6

The structural configuration of the midship section of the ship in the present study is represented in *Figure 3.1*.

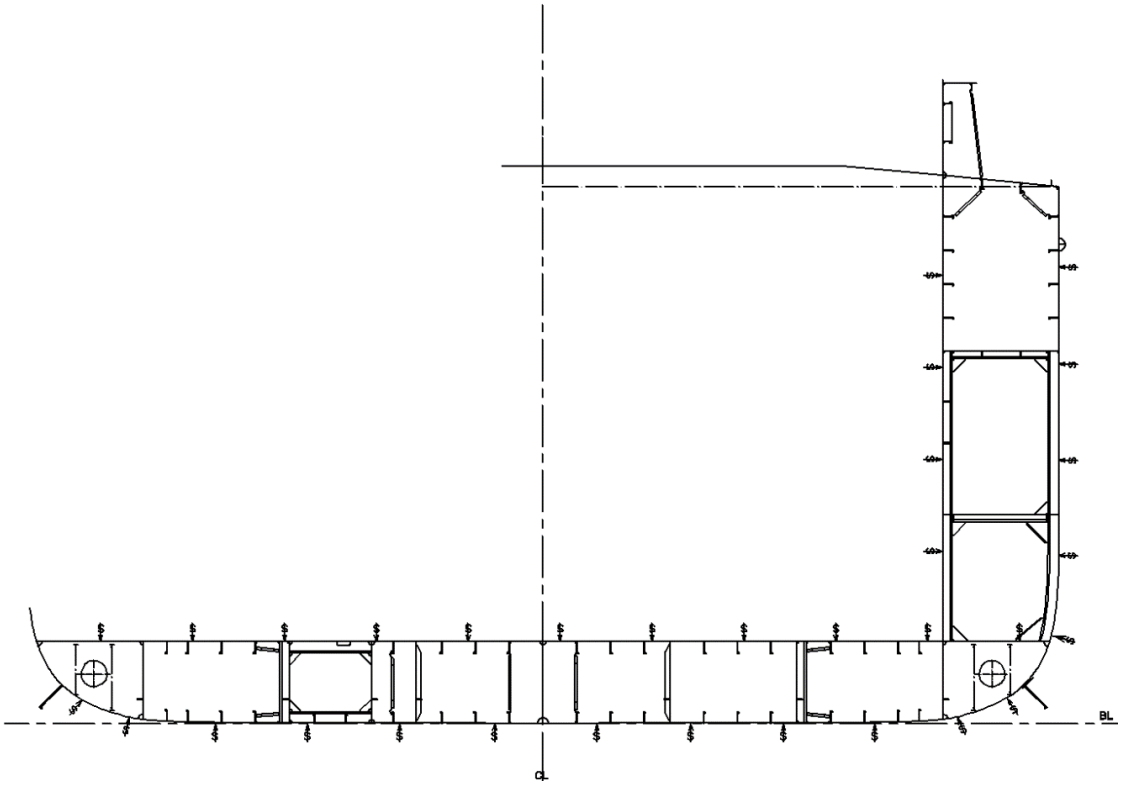

Figure 3.1 – Midship section configuration.

Considering the typical structural configuration of a multipurpose ship, shown in *Figure 3.1*, the midship section is designed according to the Rules of the classification society Bureau Veritas (BV, 2019): NR 467 Rules for Classifications of Steel Ships, July 2019 edition.

3.2 Structure design principle

Since the midship section is not symmetrical in the bottom structure, it is necessary to consider the plates and profiles of the entire section. To understand and analyse the section study more efficiently, it was decided to divide it into panels. The section was divided into nine panels of code defined by the *MARS 2000 software*: keel, bottom, inner bottom, double bottom girder, bilge, side shell, inner hull, double hull girder, and strength deck. The code of panels can be seen in *Figure 3.2*.

Figure 3.2 - Division of section by panels.

Assuming the structural configuration of *Figure 3.1*, the width of plates and the spacing of ordinary stiffeners, it is necessary to determine the longitudinal girder span. Typically, It is considered that the longitudinal girder span is three to five times the standard frame spacing. Due to the weight distribution of the vessel and the high cargo capacity to which the vessel is subject, in this particular case, it is assumed that:

$$l = 2.S \tag{3.1}$$

where S is the standard frame spacing.

The spacing of frames is not to exceed the standard frame spacing:

$$S = 2.08.L + 438\ [mm]\ for\ L < 270m \tag{3.2}$$

$$S = 1\,000\ [mm]\ for\ 270 < L < 427m \tag{3.3}$$

where L is the Rule length of the ship.

So, the standard frame spacing and the longitudinal girder span used are shown in *Table 3.2*.

Table 3.2 – Standard frame spacing and longitudinal girder span.

S_{rule}, [m]	0.68
S_{used}, [m]	0.65
l, [m]	1.30

The navigation area to which the ship is subject is the unrestricted navigation zone. The navigation coefficients used for the corresponding zone are found in *Table 3.3*.

Table 3.3 – Navigation coefficient for unrestricted navigation zone.

n	1.00
n_1	1.00

Ordinary-strength steel was selected for the bottom structure and elements of the structure closest to the neutral axis. The choice of high-tensile steel for the structural elements distant from the neutral axis, in this case, the deck area, is due to the significant stresses they are subjected to. *Figure* 3.3 shows the steel choice suitable for each structure element.

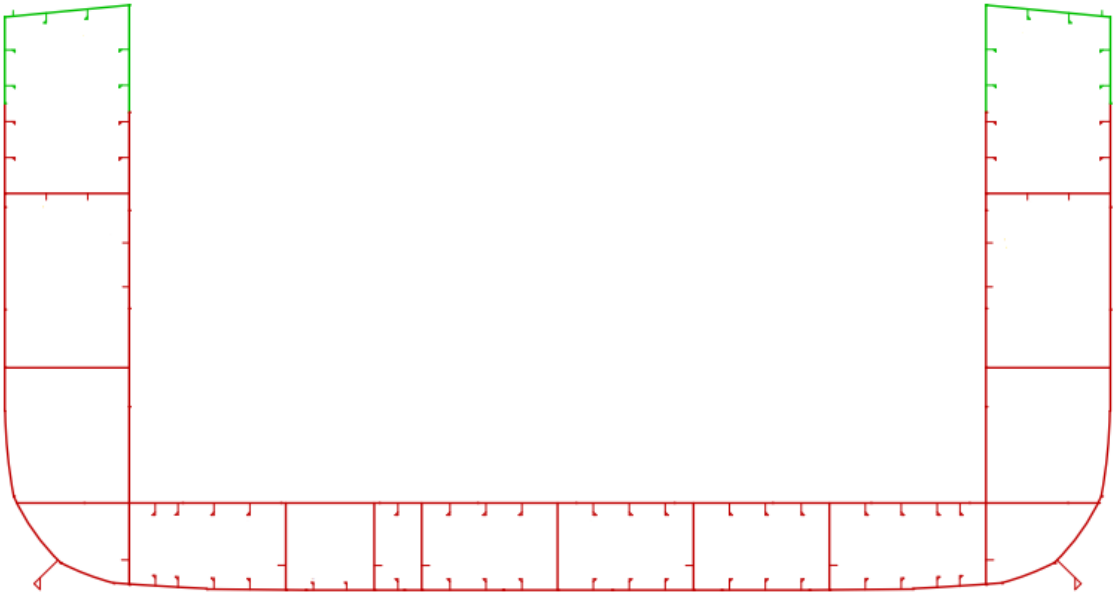

Figure 3.3 – Type of material for each element of the structure.

The Young's modulus and Poisson's ratio of the selected steel are in *Table 3.4*.

Table 3.4 – Young's modulus and Poisson's ratio of the material.

Young's Modulus, E [N/mm^2]	206 000
Poisson's Ratio, ν [-]	0.3

The mechanical properties that are the minimum yield stress R_{eH}, the ultimate minimum tensile strength R_m and material factor K of the selected steels for the ship's construction are in *Table 3.5*.

Table 3.5 – Mechanical properties of hull steels.

Steel Grades t ≤ 100mm	$R_{eH}[N/mm^2]$	$R_m[N/mm^2]$	K[-]
A-B-C-D	235	400-520	1.0
AH32-DH32-EH32-FH32	315	440-570	0.78

According to the BV, 2019 Rules defined at the beginning of this chapter, the thicknesses of the plates and scantlings to be determined in the next sub-chapters do not contain the margin of corrosion. That is, the net thickness is determined. The corrosion margins for each type of compartment are given in *Table 3.6*.

Table 3.6 – Corrosion additions $t_c, in\ mm$.

Compartment Type		General	Special Cases
Ballast Tank		1.00	1.25 in upper zone
Dry Bulk Cargo	General	1.00	-
	Inner bottom plating Inner side plating	1.75	-
	Frames, Ordinary Stiffeners and Primary Supporting Members	1.00	1.50 in the lower zone

In *Table 3.6*, “the Upper zone means the area within 1.5m below the top of the tank, and the lower zone means the area within 3m above the bottom of the tank or the hold” (BV, 2019 Rules).

“For an internal member within a given compartment, or for plating forming the boundary between two compartments of the same type, the corrosion addition being considered twice the value specified in *Table 3.6*. When a structural element is affected by more than one value of corrosion additions, the scantling criteria are applicable at the lowest point of the element “(BV, 2019 Rules).

According to the *GRABLOADING* classification notation, an additional thickness of 2 mm should be added to the thickness of the inner bottom plate panel (BV, 2019 Rules).

3.3 Hull girder loads

The moments imposed on the ship can be divided into two components: the moments created due to the shape of the ship's weights arrangement (still water bending moments) and moments created by waves (wave bending moment).

The sign conventions of bending moments and shear forces at any ship's transverse section are shown in *Figure 3.4*.

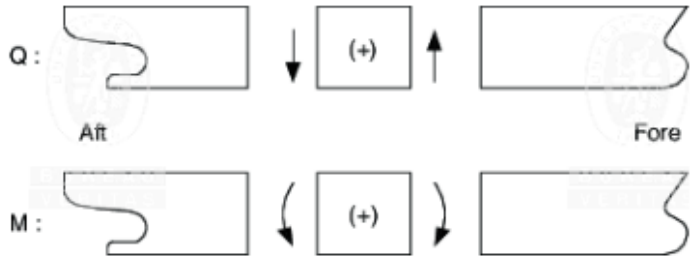

Figure 3.4 – Sign conventions for shear forces and bending moments (BV 2019 Rules).

3.3.1 Still water bending moment

At a preliminary design stage, the design still water bending moments are not defined but can be considered the longitudinal distributions at any transverse hull section shown in *Figure 3.5*.

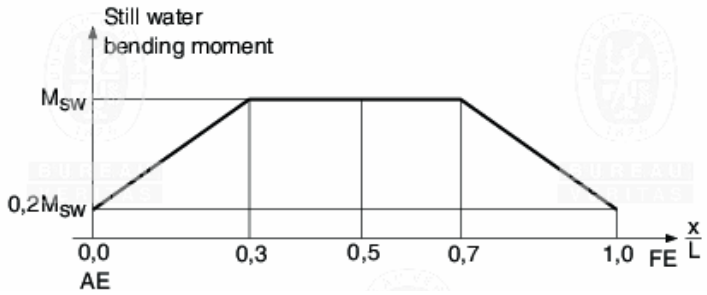

Figure 3.5 – Longitudinal distribution at a preliminary still water bending moment (BV 2019 Rules).

The design still water bending moment, in hogging or sagging conditions are obtained, in *kN.m*, from the following formulae:

$$M_{SWM,H} = 175.n_1.C.L^2.B.(C_B + 0.7).10^{-3} - M_{WV,H} \quad (3.4)$$

$$M_{SWM,S} = 175.n_1.C.L^2.B.(C_B + 0.7).10^{-3} + M_{WV,S} \quad (3.5)$$

where $M_{WV,S}$ and $M_{WV,H}$ are the vertical wave bending moments in *kN.m*, and C is the wave coefficient given as:

$$C = 10.75 - (\frac{300 - L}{100})^{1.5} \quad (3.6)$$

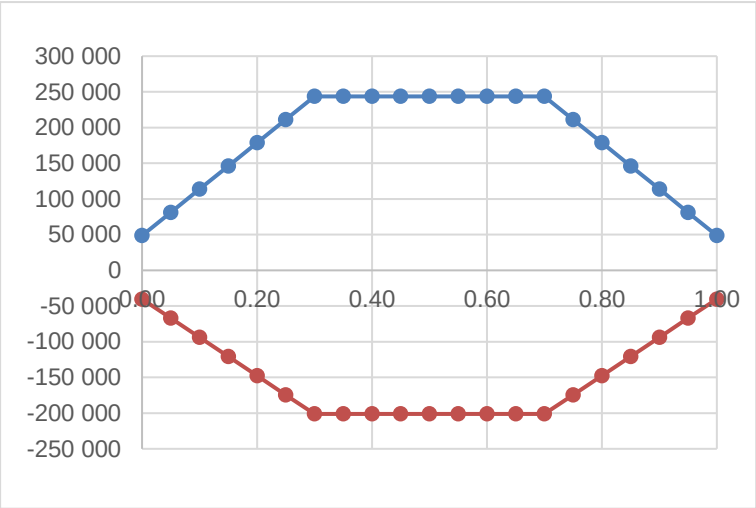

Figure 3.6 - Classification Societies Rules, Still Water Bending Moment, M_{SW} [kN.m].

3.3.2 Vertical and horizontal wave bending moment

The longitudinal distributions at any transverse hull section (F_M) for vertical and horizontal wave bending moments are shown in *Figure 3.7* may be considered.

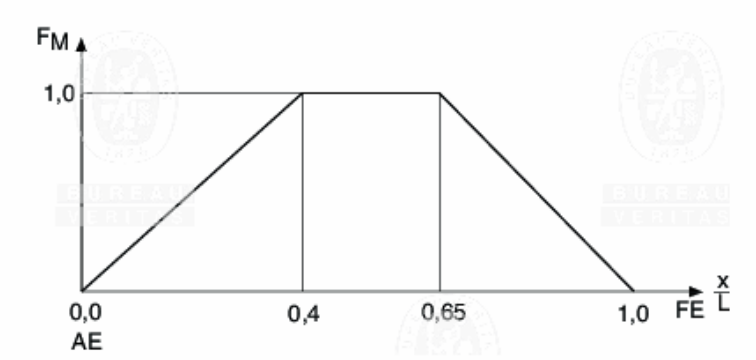

Figure 3.7 – Longitudinal distributions for vertical and horizontal wave bending moments (BV 2019 Rules).

The vertical wave bending moment in hogging or sagging conditions are obtained, in *kN.m*, from the following formulae:

$$M_{WV,H} = 190.F_M.n.C.L^2.B.C_B.10^{-3} \quad (3.7)$$

$$M_{WV,S} = -110.F_M.n.C.L^2.B.(C_B + 0.7).10^{-3} \quad (3.8)$$

The horizontal wave bending moment are obtained, in *kN.m*, from the following formula:

$$M_{WH} = 0.42.F_M.n.H.L^2.T.C_B \quad (3.9)$$

where *H* is the wave parameter given as:

$$H = 8.13 - \left(\frac{250 - 0.7.L}{125}\right)^3 \quad (3.10)$$

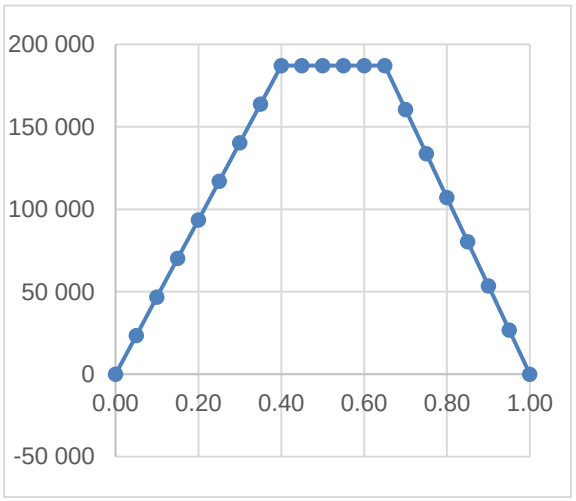

Figure 3.8 – Classification Societies Rules, Horizontal Wave Bending Moment, M_{WH} [kN.m].

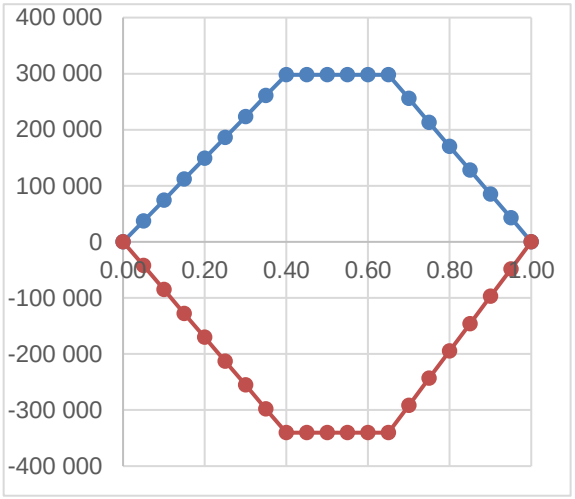

Figure 3.9 – Classification Societies Rules, Vertical Wave Bending Moment, M_{WV} [kN.m].

3.3.3 Wave torque

The wave torque is to be calculated considering the ship in two different conditions:

- Condition 1: ship direction forms an angle of 60º with the prevailing sea direction.
- Condition 2: ship forming an angle of 120º with prevailing sea direction.

The longitudinal distribution factors F_{TM} and F_{TQ} at any hull transverse section for ship conditions, 1 and 2 are shown in *Figure 3.10,* and *Figure 3.11* may be considered.

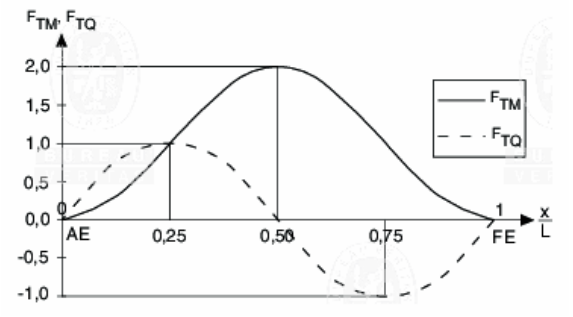

Figure 3.10 - Distribution factors for ship conditions 1 (BV 2019 Rules).

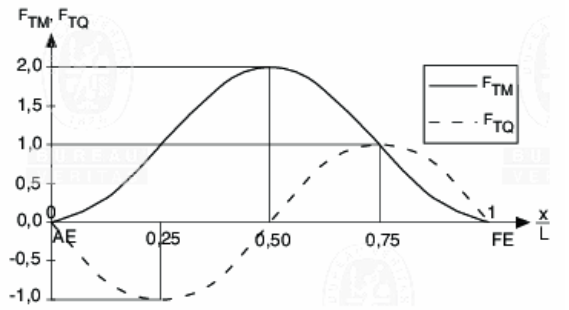

Figure 3.11 - Distribution factors for ship conditions 2 (BV 2019 Rules).

The wave torque is obtained, in *kN.m*, from the following formula:

$$M_{WT} = \frac{HL}{4}.n.\left(F_{TM}.C_M + F_{TQ}.C_Q.d\right) \quad (3.11)$$

where C_M is the wave torque coefficient, C_Q is the horizontal wave shear coefficient, and *d* is the vertical distance from the centre of torsion to a point located $0.6.T$ above the baseline.

The wave torque coefficient, C_M is defined as:

$$C_M = 0.45.B^2.C_W^2 \tag{3.12}$$

where C_W is the waterplane coefficient, not more significant than the value obtained from the following formula. The value of the block coefficient, C_B is to be assumed not less than 0.6.

$$C_W = 0.165 + 0.95.C_B \tag{3.13}$$

The horizontal wave shear coefficient, C_Q is defined as:

$$C_Q = 5.T.C_B \tag{3.14}$$

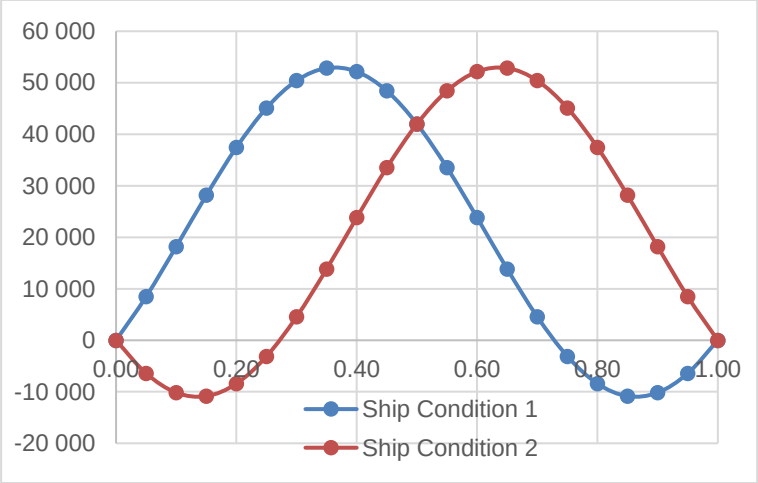

Figure 3.12 - Classification Societies Rules, Wave Torque, M_{WT} [kN.m].

3.3.4 Vertical wave shear force

The longitudinal distributions at any transverse hull section (F_Q) for positive and negative shear forces are shown in *Figure 3.13* may be considered.

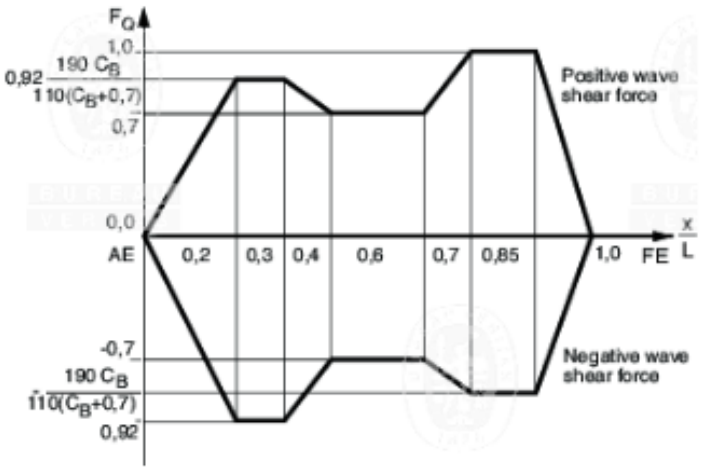

Figure 3.13 – Longitudinal distributions for positive and negative shear forces (BV 2019 Rules).

The vertical wave shear force is obtained, in *kN*, from the following formula:

$$Q_{WV} = 30.F_Q.n.C.L.B.(C_B + 0.7).10^{-2} \quad (3.15)$$

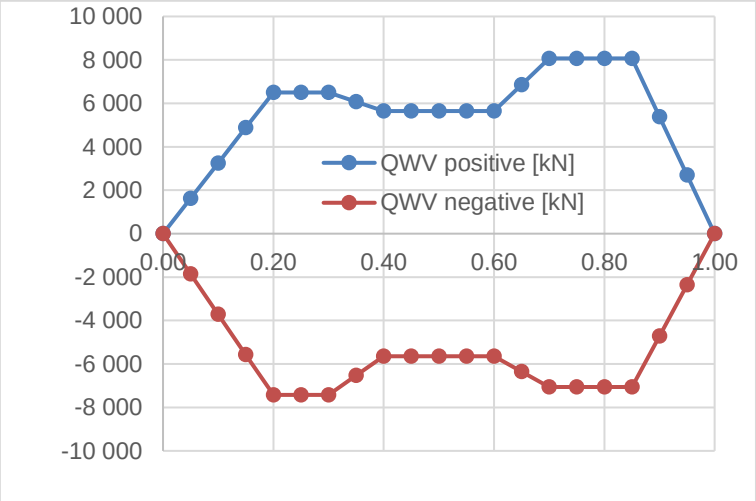

Figure 3.14 - Classification Societies Rules, Vertical Wave Shear Force, Q_{WV} [kN].

3.4 Ship motions and accelerations

According to the established Rules indicated at the beginning of this chapter, ship motions and accelerations are assumed to be periodic. The motion amplitudes are half of the crest to through amplitudes.

3.4.1 Ship absolute motions and accelerations

According to the established rules, the ship's absolute motions and acceleration of a midship section are presented in *Table 3.7*.

Table 3.7 – Ship motions and accelerations (BV, 2019 Rules).

Ship motion or acceleration	Acceleration	Period [s]	Amplitude [rad]
Surge	$a_{SU} = 0.50\,[m/s^2]$	-	-
Sway	$a_{SW} = 0.775 a_B.g\,[m/s^2]$	$T_W = \frac{0.8\sqrt{L}}{1.22F+1}$	-
Heave	$a_H = a_B.g\,[m/s^2]$	-	-
Roll	$\alpha_R = A_R.(\frac{2.\pi}{T_R})^2\,[rad/s^2]$	$T_R = 2.2.\frac{\delta}{\sqrt{GM}}$	$A_R = a_B.\sqrt{E}$
Pitch	$\alpha_p = A_p.(\frac{2.\pi}{T_p})^2\,[rad/s^2]$	$T_p = 0.575\sqrt{L}$	$A_p = 0.328 a_B.(1.32 - \frac{h_W}{L}).(\frac{0.6}{C_B})^{0.75}$

Yaw	$\alpha_Y = 1.581.\frac{a_B.g}{L}\ [rad/s^2]$	-	-

In *Table 3.7*:

$\boldsymbol{a_B}$ is the motion and acceleration parameter:

$$a_B = n.(0.76F + 1.875.\frac{h_W}{L}) \tag{3.16}$$

$\boldsymbol{h_W}$ is the wave parameter, in *m*:

$$h_W = 11.44 - |\frac{L-250}{110}|^3 \ for\ L < 350\ m \tag{3.17}$$

F is the Froude's number:

$$F = \frac{0.164.V}{L^{0.5}} \tag{3.18}$$

E is the coefficient to be taken not less than 1.0:

$$E = 1.39.\frac{GM}{\delta^2}.B \tag{3.19}$$

where *GM* is the distance from the ship's centre of gravity to the transverse metacentre, in m, (assumed that *GM* = 0.07*B* for full load and *GM* = 0.18*B* for Ballast condition), and $\boldsymbol{\delta}$ is the roll radius of gyration, in *m*, (assumed that $\boldsymbol{\delta = 0.35B}$).

3.4.2 Ship relative motions and acceleration

Ship relative motions and accelerations are to be calculated considering the ship in the following conditions:

- Upright ship condition.
- Inclined ship condition.

In the upright ship conditions, the ship encounters waves that produce the following ship motions: surge, heave and pitch. In the inclined ship condition, the ship encounters waves that produce the following ship motions: sway, roll, and yaw (BV, 2019 Rules).

The reference value of the relative motion $\boldsymbol{h_1}$ in the upright ship condition, in *m*, at the midship section, is obtained from the following formula:

$$h_1 = 0.42.n.C.(C_B + 0.7) \tag{3.20}$$

where *n* is the navigation coefficient, and *C* is the wave parameter.

The reference value of the relative motion in the inclined ship condition $\boldsymbol{h_2}$, in *m*, at the midship section, is obtained from the following formula:

$$h_2 = 0.5.h_1 + A_R.\frac{B_W}{2} \tag{3.21}$$

where A_R is the roll amplitude, in rad, and B_W is the moulded breadth, in m, measured at the waterline at draught T_1.

The values of $\boldsymbol{h_1}$ and $\boldsymbol{h_2}$ cannot be greater than the minimum of $\boldsymbol{T_1}$ and $\boldsymbol{D - 0.9T}$.

For upright and inclined ship conditions, the value of the longitudinal, transversal, and vertical accelerations is obtained from the formulae in *Table 3.8*.

Table 3.8 – Reference values of the longitudinal, transversal and vertical accelerations (BV, 2019 Rules).

Direction	Upright Ship Condition	Inclined Ship Condition
Longitudinal (X)	$\mathbf{a_{X1}} = \sqrt{\mathbf{a_{SU}^2} + [\mathbf{A_p}.\mathbf{g} + \boldsymbol{\alpha}_\mathbf{p}(\mathbf{Z} - \mathbf{T_1})]^2}$	$\mathbf{a_{X2}} = \mathbf{0}$
Transverse (Y)	$\mathbf{a_{Y1}} = \mathbf{0}$	$\mathbf{a_{Y2}} = \sqrt{\mathbf{a_{SW}^2} + [\mathbf{A_R}.\mathbf{g} + \boldsymbol{\alpha}_\mathbf{R}(\mathbf{Z} - \mathbf{T_1})]^2 + \boldsymbol{\alpha}_\mathbf{Y}^2.\mathbf{K_x}.\mathbf{L^2}}$
Vertical (Z)	$\mathbf{a_{Z1}} = \sqrt{\mathbf{a_H^2} + \boldsymbol{\alpha}_\mathbf{p}^2.\mathbf{K_x}.\mathbf{L^2}}$	$\mathbf{a_{Z2}} = \sqrt{\mathbf{0.25}.\mathbf{a_H^2} + \boldsymbol{\alpha}_\mathbf{R}^2.\mathbf{y^2}}$

where $\boldsymbol{K_x}$ is defined as:

$$K_x = 1.2(\frac{X}{L})^2 - 1.1.\frac{X}{L} + 0.2 \quad (3.22)$$

The value of $\boldsymbol{K_x}$ cannot be less than 0.018.

3.5 Load cases

The load cases used for structural element analysis are:

- Load cases “a” and “b”.
- Load cases “c” and “d”.

Load cases “a” and “b” refer to the ship in upright conditions, i.e., at rest or having surge, heave, and pitch motions. The wave loads and relative motions of the ship present in load cases “a” and “b” can be shown in *Figure 3.15* and *Figure 3.16*, respectively.

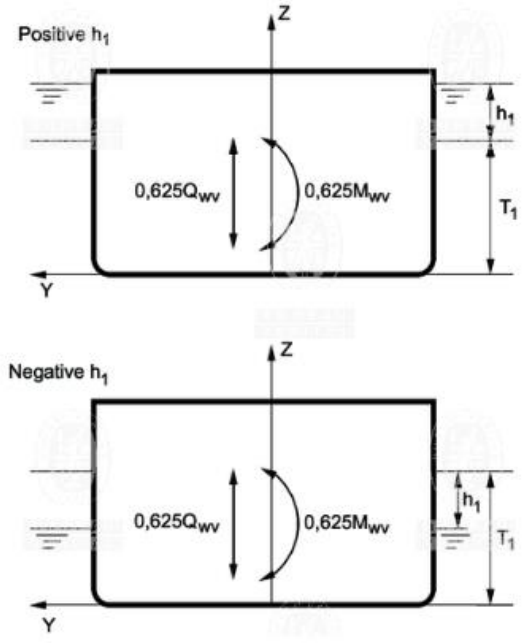

Figure 3.15 - Wave loads in load case "a" (BV 2019 Rules).

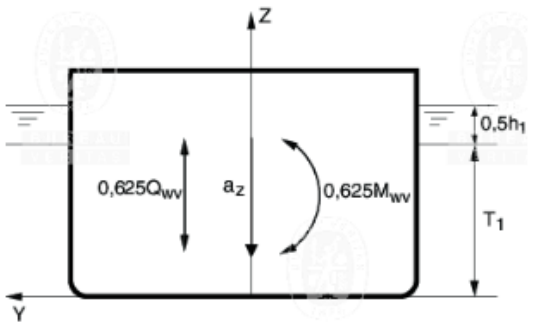

Figure 3.16 - Wave loads in load case "b" (BV 2019 Rules).

Load cases "c" and "d" refer to the ship in inclined conditions, i.e., sway, roll and yaw motions. The wave loads and relative motions of the ship present in load cases "c" and "d" can be shown in *Figure 3.17* and *Figure 3.18,* respectively.

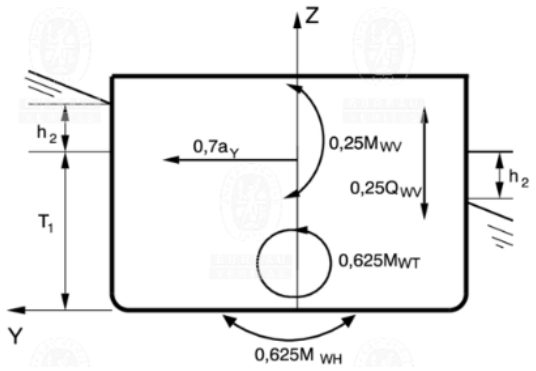

Figure 3.17 - Wave loads in load case "c" (BV 2019 Rules).

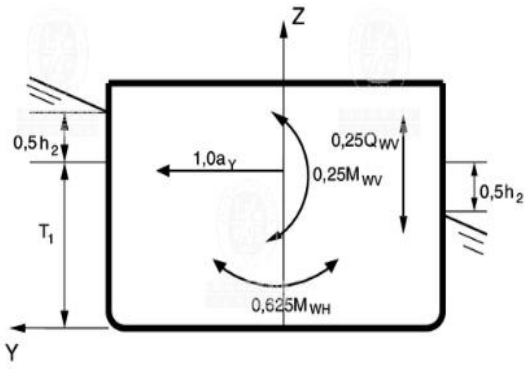

Figure 3.18 - Wave loads in load case "d" (BV 2019 Rules).

3.6 Sea pressures

3.6.1 Still water pressures

The still water pressure on the sides and bottom, at any point of the hull, in kN/mm^2 is obtained from the formulae in *Table 3.9* and shown in *Figure 3.19*.

Table 3.9 – Still water pressure on sides and bottom (BV, 2019 Rules).

Location	Still water pressure $p_s \; in \; kN/m^2$
$Z \leq T_1$	$\rho . g . (T_1 - Z)$
$Z > T_1$	0

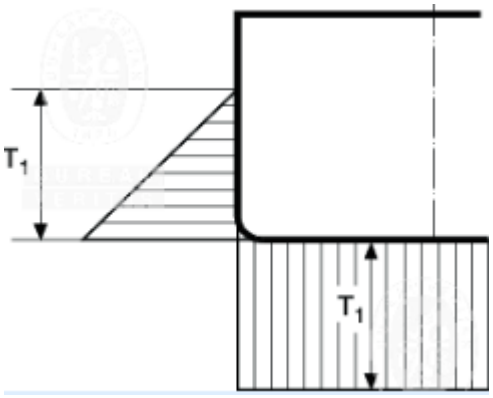

Figure 3.19 – Still water pressure (BV 2019 Rules).

The still water pressure on exposed decks, in kN/mm^2, is obtained from the following formula:

$$P_d \; = \; 10 . \varphi_1 . \varphi_2 \tag{3.23}$$

where φ_1 is the coefficient of exposed deck location (in this case $\varphi_1 \; = \; 1$ for freeboard deck and below) and φ_2 is taken equal to: $\varphi_2 \; = \; \frac{L}{120}$.

3.6.2 Wave pressures

The wave pressure at any point of the bottom and side for upright ship condition is obtained from the formulae in *Table 3.10* and shown in *Figure 3.20* for load case “a” and *Figure 3.21* for load case “b”.

Table 3.10 – Wave pressures on bottom and side for upright ship conditions (load cases “a” and “b”), (BV, 2019 Rules).

Location	Wave pressure $p_W \; in \; kN/m^2$	
	Crest	Trough
$Z \leq T_1$	$\rho . g . h . e^{\frac{-2.\pi . (T_1 - Z)}{L}}$	$- \rho . g . h . e^{\frac{-2.\pi . (T_1 - Z)}{L}}$
$Z > T_1$	$\rho . g . (T_1 + h - Z)$	0.0

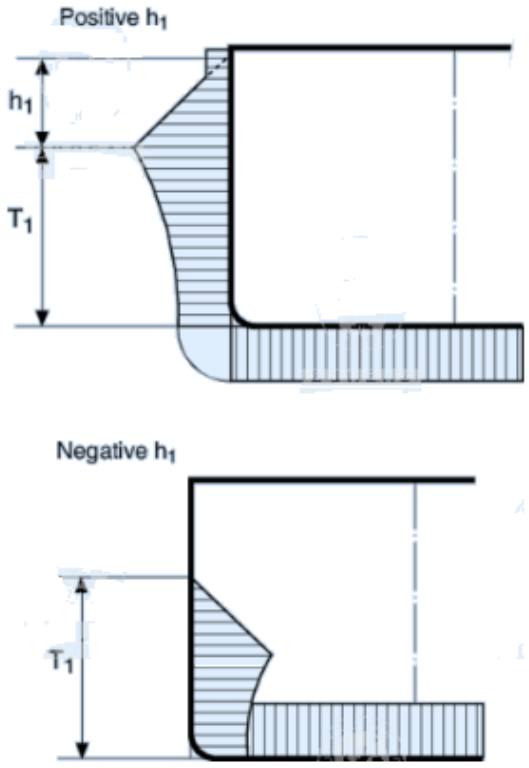

Figure 3.20 – Wave pressure in load case "a" (BV 2019 Rules).

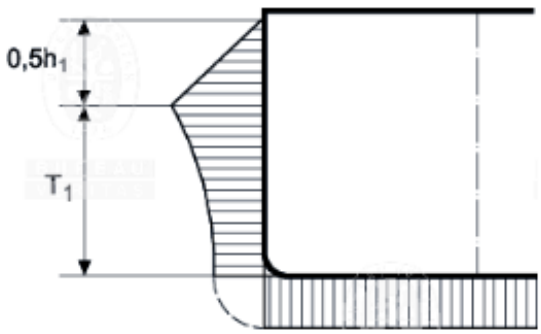

Figure 3.21 – Wave pressure in load case "b" (BV 2019 Rules).

The wave pressure at any point of the bottom and side for inclined ship condition is obtained from the formulae in *Table 3.11* and shown for load case "c" and load case "d".

Table 3.11 – Wave pressure on bottom and side for inclined ship conditions (load cases "c" and "d"), (BV, 2019 Rules).

Location	Wave pressure $p_W, in\ kN/m^2$	
	$y \geq 0$	$y < 0$
$Z \leq T_1$	$\beta . C_{F2} . \rho . g . \left[\frac{y}{B_W} . h_1 . e^{\frac{-2.\pi.(T_1 - Z)}{L}} + A_R . y . e^{\frac{-\pi.(T_1 - Z)}{L}} \right]$	$\beta . C_{F2} . \rho . g . \left[\frac{y}{B_W} . h_1 . e^{\frac{-2.\pi.(T_1 - Z)}{L}} + A_R . y . e^{\frac{-\pi.(T_1 - Z)}{L}} \right]$
$Z > T_1$	$\rho . g . \left[T_1 + \beta . C_{F2} . \left(\frac{y}{B_W} . h_1 + A_R . y \right) - Z \right]$	0.0

where C_{F2} is the combination factor, to be taken equal to: $C_{F2} = 1$ for load case "c" and $C_{F2} = 0.5$ for load case "d".

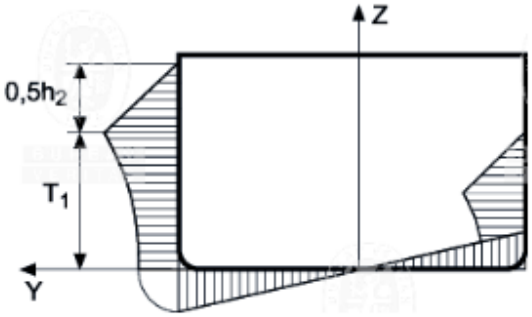

Figure 3.22 - Wave pressure in load case "c" (BV 2019 Rules).

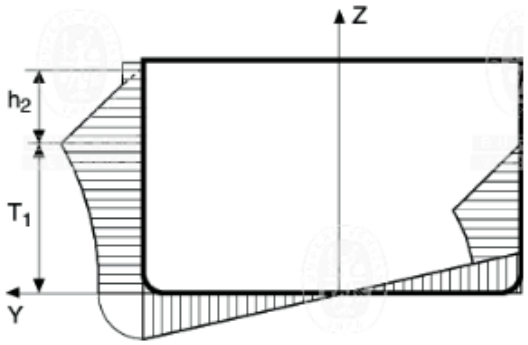

Figure 3.23 - Wave pressure in load case "d" (BV 2019 Rules).

The pressure for exposed decks is to be considered independently of the pressures due to dry uniform cargoes. The still water pressure on the exposed deck is defined in *Subchapter 3.6.1*.

The wave pressure on the exposed deck due to the green sea is obtained from the formulae in *Table 3.12* for upright ship conditions (load cases "a" and "b") and *Table 3.13* for inclined ship conditions (load cases "c" and "d").

Table 3.12 – Wave pressure on exposed deck for upright ship conditions (load cases "a" and "b"), (BV, 2019 Rules).

Location	Wave pressure $p_W, in\ kN/m^2$	
	$y \geq 0$	$y < 0$
Exposed Deck	$0.4.\rho.g.\left[T_1 + \beta.C_{F2}.\left(\frac{y}{B_W}.h_1 + A_R.y\right) - Z\right]$	0.0

Table 3.13 – Wave pressure on exposed deck for inclined ship conditions (load cases "c" and "d"), (BV, 2019 Rules).

Location	Wave pressure $p_W, in\ kN/m^2$	
	Crest	Through
Exposed Deck	$17.5.n.\varphi_1.\varphi_2$	0.0

3.7 Internal sea pressures and forces

To determine the ship's internal sea pressures and forces, it is necessary to define which compartments to consider in the study of the design of the midship section. *Figure 3.24* shows the compartments in question.

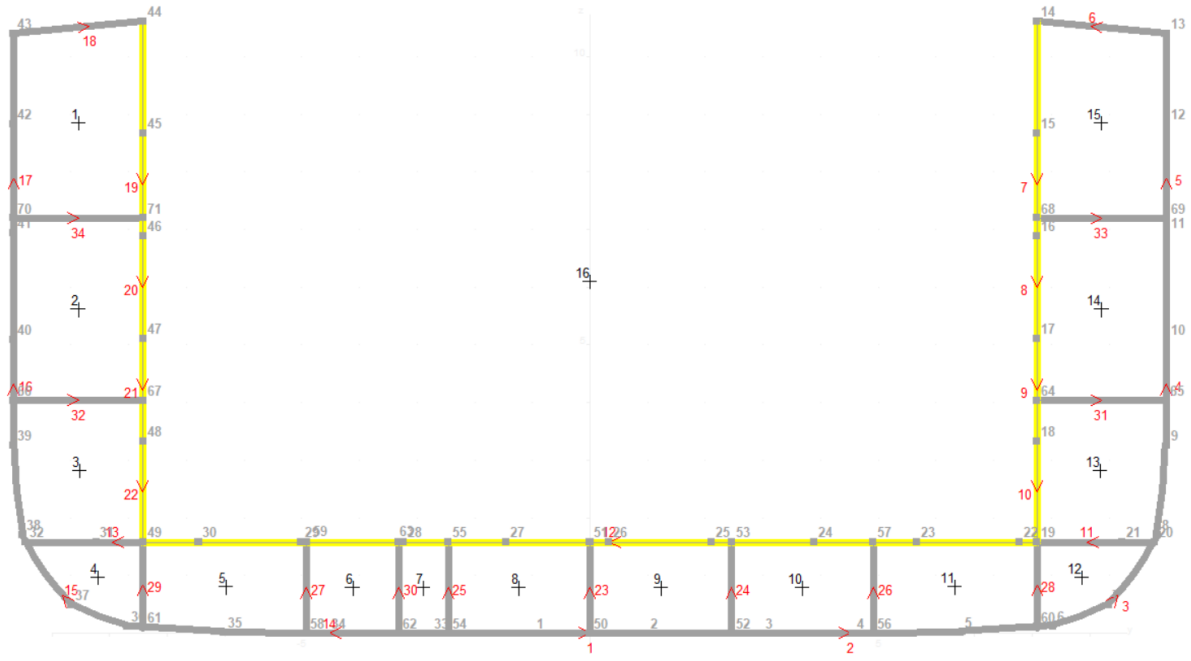

Figure 3.24 – Compartments of midship section.

In compartment 16, i.e., in the cargo hold, it is assumed that the maximum permissible load is 15 t/m^2(150 kN/m^2). The double bottom and double hull compartments are assumed to be empty ballast tanks. Compartment 12 of the double bottom is considered a tunnel for the passage of piping.

3.8 Hull girder strength

Hull girder transverse sections are to be considered constituted by the members contributing to the hull girder longitudinal strength, i.e., all continuous longitudinal members below the strength deck.

3.8.1 Normal stresses

The normal stresses at any point of the transverse hull section induced by vertical bending moment are obtained in N/mm^2, from the following formula:

$$\sigma_1 = \frac{M_{SW} + M_{WV}}{Z_A} . 10^{-3} \tag{3.24}$$

where $Z_A[m^3]$ is the gross section modulus at any point of the transverse hull section.

The normal stresses at the bottom and deck, in N/mm^2, are obtained from the following formulae:

$$\sigma_1 = \frac{M_{SW} + M_{WV}}{Z_{AB}} . 10^{-3} \tag{3.25}$$

$$\sigma_1 = \frac{M_{SW} + M_{WV}}{Z_{AD}} . 10^{-3} \tag{3.26}$$

where $Z_{AB}[m^3]$ and $Z_{AD}[m^3]$ are the gross section modulus at the bottom and deck, respectively.

Since the ship has large openings in the strength deck, the normal stresses induced by moments of torque and bending moments must be considered. The normal stresses are obtained in N/mm^2, from the following formula:

$$\sigma_1 = \{\frac{M_{SW}}{Z_A} + \frac{0.4. M_{WV}}{Z_A} + \frac{M_{WH}}{I_Z}|y|\}. 10^{-3} + \sigma_\Omega \tag{3.27}$$

where σ_Ω is the warping stress in N/mm^2, induced by the torque.

The normal stresses σ_1 is to be checked according to the following formula:

$$\sigma_1 \leq \sigma_{1,ALL} \tag{3.28}$$

where $\sigma_{1,ALL}[N/mm^2]$ is the allowable normal stress given as:

$$\sigma_{1,ALL} = \frac{175}{k} \tag{3.29}$$

3.8.2 Shear stresses

The shear stresses induced by the vertical shear forces for ships without effective longitudinal bulkheads are obtained in N/mm^2, from the following formula:

$$\tau_1 = (Q_{SW} + Q_{WV} - \varepsilon \Delta Q_C)\frac{S}{I_y t}\delta \tag{3.30}$$

where *t* is the minimum thickness, in *mm*, of side and inner side plating; δ is the shear distribution coefficient; ΔQ_C is the shear force correction; *S* is the first moment, in m^3, of the transverse hull section and $\varepsilon = sgn(Q_{SW})$.[1]

[1] *sgn* is a mathematical function that extracts the sign of a real number. The sign function of a real number *a* is defined as:

$$sgn(a) = \begin{cases} -1 \; if \; a < 0 \\ 0 \; if \; a = 0 \\ 1 \; if \; a > 0 \end{cases}$$

The shear distribution coefficient δ is obtained from *Table 3.14*.

Table 3.14 – Shear stresses induced by vertical shear forces (BV, 2019 Rules).

Ship typology	Location	T [*mm*]	δ	
Double-side ships without effective longitudinal bulkheads (See *Figure 3.25*)	Sides	t_S	$\frac{(1-\Phi)}{2}$	$\Phi = 0.275 + 0.25\,\alpha\alpha = \frac{t_{ISM}}{t_{SM}}$
	Inner Sides	t_{IS}	$\frac{\Phi}{2}$	

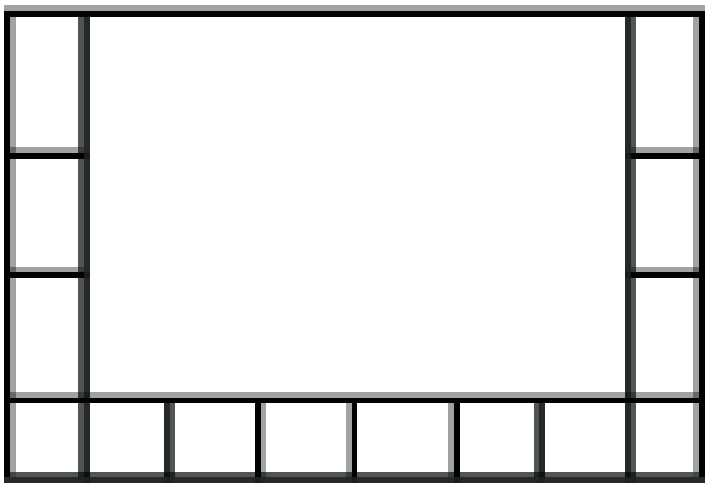

Figure 3.25 - Ship typology (BV 2019 Rules).

The shear stresses τ_1 is to be checked according to the following formula:

$$\tau_1 \leq \tau_{1,ALL} \tag{3.31}$$

where $\tau_{1,ALL}[N/mm^2]$ is the allowable shear stress given as:

$$\tau_{1,ALL} = \frac{110}{k} \tag{3.32}$$

3.8.3 Section modulus and moment of inertia

The minimum hull girder section modulus required to ensure enough hull girder rigidity are to be not less than the greater value obtained, in m^3, from the following formulae:

$$Z_{R,MIN} = n_1.C.L^2.B.(C_B + 0.7).k.10^{-6} \tag{3.33}$$

(3.34)

$$Z_R = \frac{M_{SW} + M_{WV}}{\sigma_{1,ALL}}.10^{-3}$$

The minimum gross midship section moment of inertia about its horizontal neutral axis required to ensure enough hull girder rigidity is to be not less than the value obtained, in m^4, from the following formula:

$$I_{YR} = 3.\frac{n}{n_1}.Z'_{R,MIN}.L.10^{-2} \quad (3.35)$$

where $Z'_{R,MIN}$ is the required midship section modulus $Z_{R,MIN}$, but assuming *k* =1.

3.8.4 Higher strength steel

The higher strength steel is used in calculating the required section modulus at the deck and is to be adopted for all members contributing to the longitudinal strength, at least up to a vertical distance, in *m*, below a horizontal line located at a distance V_D, can be obtained from the following formula:

$$V_{HD} = \frac{\sigma_{1D} - k.\sigma_{1,ALL}}{\sigma_{1B} + \sigma_{1D}}.(N + V_D) \quad (3.36)$$

where σ_{1D} and σ_{1B} are the normal stresses at the bottom and deck, respectively; N is the neutral axis and V_D is the vertical distance, in *m*, given as:

$$V_D = Z_D - N \quad (3.37)$$

where Z_D is the Z coordinate, in *m*, of the strength deck.

3.9 Hull scantlings

3.9.1 Plating

According to the classification society, the thickness calculated in this subchapter are net, i.e., they do not include any margin for corrosion (t_c). The margin for corrosion was defined in *Subchapter 3.2*.

The gross thickness is obtained, in *mm*, from the following formula:

$$t_{gross} = t_{net} + t_c \quad (3.38)$$

The partial safety factors to be considered for checking the plating are specified in *Table 3.15*.

Table 3.15 – Partial safety factors for plating subjected to lateral pressure (BV, 2019 Rules).

Still water hull girder loads, γ_{S1}	1.00
Wave hull girder loads, γ_{W1}	1.15

Still water pressures, γ_{S2}	1.00
Wave pressures, γ_{W2}	1.20
Material, γ_m	1.02
Resistance, γ_R	1.20

The net thickness of the plating is to be not less than the values given in *Table 3.16*. For the bilge plating, the net thickness is to be not less than the actual thickness of the adjacent bottom or side plating, whichever is greater.

Table 3.16 – Minimum net thickness of plating, in mm (BV, 2019 Rules).

Plating	Minimum net thickness [*mm*]
Keel	$3.8 + 0.040.L.k^{\frac{1}{2}} + 4.5.s$
Bottom	$1.9 + 0.032.L.k^{\frac{1}{2}} + 4.5.s$
Inner Bottom	$3.0 + 0.024.L.k^{\frac{1}{2}} + 4.5.s$
Side	$2.1 + 0.031.L.k^{\frac{1}{2}} + 4.5.s$
Inner Side	$1.7 + 0.013.L.k^{\frac{1}{2}} + 4.5.s$
Weather Strength Deck	$1.6 + 0.032.L.k^{\frac{1}{2}} + 4.5.s$
Centre Girder	$2.0.L^{\frac{1}{3}}.k^{\frac{1}{6}}$
Side Girders	$1.4.L^{\frac{1}{3}}.k^{\frac{1}{6}}$

It is considered that the elementary plate panel is the smallest unstiffened part of plating. The loading point considered for calculating lateral pressure and hull girder stresses are at the lower edge of the elementary plate panel or the point of minimum y-value among those of the elementary plate panel considered in the case of horizontal plating (BV, 2019 Rules).

The net thickness of the plate panel subjected to in-plane normal stresses acting on the shorter side is to be not less than the value obtained, in mm, from the following formula:

$$t = 14.9.C_a.C_r.S.\sqrt{\gamma_R.\gamma_{m.}\frac{\gamma_{S2}.p_S + \gamma_{W2}.p_W}{\lambda_L.R_y}} \quad (3.39)$$

where: p_S is the still water pressure and p_w is the wave pressure, *s* is the shorter side of plating, and l is the longer side of plating, C_a is the aspect ratio of the plate panel *(3.40)*, C_r is the coefficient of curvature *(3.41)* and R_y is the minimum yield stress *(3.42)*.

$$C_a = 1.21.\sqrt{1 + 0.33.(\frac{s}{l})^2} - 0.69.\frac{s}{l} \quad (3.40)$$

$$C_r = 1 - 0.5.\frac{s}{r} \quad (3.41)$$

$$R_y = \frac{R_{eH}}{k} \quad (3.42)$$

The coefficient λ_L is given by:

$$\lambda_L = \sqrt{1 - 3(\gamma_m.\frac{\tau_1}{R_y})^2 - 0.95.(\gamma_m.\frac{\sigma_{x1}}{R_y})^2} - 0.225.\gamma_m.\frac{\sigma_{x1}}{R_y} \quad (3.43)$$

where σ_{x1} is the in-plane hull girder normal stresses, in N/mm^2, and τ_1 is the in-plane hull girder shear stresses, in N/mm^2.

The in-plane hull girder normal stresses, σ_{x1}, is given by:

$$\sigma_{x1} = \gamma_{S1}\sigma_{S1} + \gamma_{W1}C_{FT}(C_{FV}\sigma_{WV1} + C_{FH}\sigma_{WH1} + C_{F\Omega}\sigma_{\Omega}) \quad (3.44)$$

where $\sigma_{S1}, \sigma_{WV1}, \sigma_{WH1}$ Are the hull girder normal stresses in N/mm^2; σ_{Ω} is the compression warping stress in N/mm^2, $C_{FV}, C_{FH}, C_{F\Omega}$ are combinations factors and C_{FT} is the reduction factor for tanks subject to flow through ballast water exchange(consider value 1.0 for normal operations).

The combination factors for each load case are presented in *Table 3.17*.

Table 3.17 – Combination factors for each load case (BV, 2019 Rules).

Load Case	C_{FV}	C_{FH}	$C_{F\Omega}$
"a"	1.0	0.0	0.0
"b"	1.0	0.0	0.0
"c"	0.4	1.0	1.0
"d"	0.4	1.0	0.0

The hull girder normal stresses $\sigma_{S1}, \sigma_{WV1}, \sigma_{WH1}$ are defined by the formulae given in *Table 3.18*.

Table 3.18 – Hull girder normal stress σ_{S1}, σ_{WV1}, σ_{WH1} (BV, 2019 Rules).

Condition	$\sigma_{S1}\ [N/mm^2]$	$\sigma_{WV1}\ [N/mm^2]$	$\sigma_{WH1}\ [N/mm^2]$
$\frac{\lvert\gamma_{S1}M_{SW,S} + 0.625\gamma_{W1}C_{FV}F_D\ M_{WV,S}\rvert}{\gamma_{S1}M_{SW,H} + 0.625\gamma_{W1}C_{FV}M_{WV,H}} \geq 1$	$\lvert\frac{M_{SW,S}}{I_Y}(z - N)\rvert 10^{-3}$	$\lvert\frac{0.625F_D M_{WV,S}}{I_Y}(z - N)\rvert 10^{-3}$	$\lvert\frac{0.625M_{WH}}{I_Z}y\rvert 10^{-3}$
$\frac{\lvert\gamma_{S1}M_{SW,S} + 0.625\gamma_{W1}C_{FV}F_D\ M_{WV,S}\rvert}{\gamma_{S1}M_{SW,H} + 0.625\gamma_{W1}C_{FV}M_{WV,H}} < 1$	$\lvert\frac{M_{SW,H}}{I_Y}(z - N)\rvert 10^{-3}$	$\lvert\frac{0.625F_D M_{WV,H}}{I_Y}(z - N)\rvert 10^{-3}$	

Note 1: $F_D = 1$

The in-plane hull girder shear stresses, τ_1 is given by:

$$\tau_1 = \gamma_{S1}\tau_{S1} + 0.625C_{FV}\gamma_{W1}\tau_{W1} \tag{3.45}$$

where τ_{S1} and τ_{W1} are the absolute value of the hull girder shear stresses in N/mm^2 induced by the maximum still water hull girder vertical shear force or induced by the maximum wave hull girder vertical shear force, respectively.

The absolute value of the hull girder shear stresses τ_{S1} and τ_{W1} are defined by the formulae given in *Table 3.19*.

Table 3.19 – Hull girder shear stresses τ_{S1} and τ_{W1} (BV, 2019 Rules).

Structural element	$\tau_{S1}, \tau_{W1}\ [N/mm^2]$
Bottom, inner bottom and decks	0
Bilge, side, inner side and longitudinal bulkheads:	
$0 \leq Z \leq 0.25D$	$\tau_0(0.5 + 2\frac{Z}{D})$
$0.25D \leq Z \leq 0.75D$	τ_0
$0.75D \leq Z \leq D$	$\tau_0(2.5 - 2\frac{Z}{D})$

Note 1: $\tau_0 = \frac{47}{k}\left\{1 - \frac{6.3}{\sqrt{L_1}}\right\}$

3.9.2 Ordinary stiffeners

The shear area and the section modulus of stiffeners calculated in this subchapter are net. The gross scantlings are obtained from the following formula:

$$W_N = W_G\,(1 - \alpha t_C) - \beta . t_C \tag{3.46}$$

where α and β are the coefficients defined in *Table 3.20*.

Table 3.20 – Coefficient α and β for different types of ordinary stiffeners (BV, 2019 Rules).

Type of ordinary stiffeners	α	β
Flat bars	0.035	2.8
Bulb: $W_G \leq 200\ cm^3$	0.070	0.4
Bulb: $W_G > 200\ cm^3$	0.035	7.4

The partial safety factors to be considered for checking ordinary stiffeners are specified in *Table 3.21*.

Table 3.21 – Partial safety factor for ordinary stiffener (BV, 2019 Rules).

Still water hull girder loads, γ_{S1}	1.00
Wave hull girder loads, γ_{W1}	1.15
Still water pressures, γ_{S2}	1.00
Wave pressures, γ_{W2}	1.20
Material, γ_m	1.02
Resistance, γ_R	1.02

The net thickness of the web of ordinary stiffeners is to be not less than the lesser of the net thickness of the attached plating or:

$$t_{MIN} = 0.8 + 0.004 . L . K^{\frac{1}{2}} + 4.5 . S \; for \; L < 120m \tag{3.47}$$

$$t_{MIN} = 1.6 + 2.2 . K^{\frac{1}{2}} + S \; for \; L \geq 120m \tag{3.48}$$

The maximum normal stress σ and shear stress τ for single-span longitudinal stiffener are to be obtained in N/mm^2, from the following formulae:

$$\sigma = \beta_b \frac{\gamma_{S2} p_s + \gamma_{W2} p_W}{mW} (1 - \frac{s}{2l}). s. l^2 10^3 + \sigma_{x1} \quad (3.49)$$

$$\tau = 5\beta_s \frac{\gamma_{S2} p_s + \gamma_{W2} p_W}{A_{sh}} (1 - \frac{s}{2l}). s. l \quad (3.50)$$

where *m* is the boundary conditions (in this case, considered *m* =12 for simply supported at both ends); *s* is the spacing between stiffeners, and *l* is the span of stiffeners; β_b and β_s are coefficients to be defined in *Table 3.22*.

Table 3.22 – Coefficients β_b and β_s (BV, 2019 Rules).

Brackets at ends	Bracket lengths	β_b	β_s
0	-	1.0	1.0

The hull girder normal stress, σ_{x1}, for longitudinal ordinary stiffeners contributing to the hull, girder longitudinal strength and subjected to lateral pressure are defined by *(3.44).*

The hull girder normal stresses σ_{S1}, σ_{WV1}, σ_{WH1} are defined by the formulae given in *Table 3.23*.

Table 3.23 – Hull girder normal stress σ_{S1}, σ_{WV1}, σ_{WH1} (BV, 2019 Rules).

Condition	$\sigma_{S1}\ [N/mm^2]$	$\sigma_{WV1}\ [N/mm^2]$	$\sigma_{WH1}\ [N/mm^2]$
Lateral pressure applied on the side opposite to the ordinary stiffener concerning the plating:			
Z ≥ N in general; Z < N for stiffeners simply supported at both ends	$\lvert\frac{M_{SW,S}}{I_Y}(Z-N)\rvert 10^{-3}$	$\lvert\frac{0.625 F_D M_{WV,S}}{I_Y}(Z-N)\rvert 10^{-3}$	
Z < N in general; Z ≥ N for stiffeners simply supported at both ends	$\lvert\frac{M_{SW,H}}{I_Y}(Z-N)\rvert 10^{-3}$	$\lvert\frac{0.625 M_{WV,H}}{I_Y}(Z-N)\rvert 10^{-3}$	$\lvert\frac{0.625 M_{WH}}{I_Z} y\rvert 10^{-3}$
Lateral pressure applied on the same side to the ordinary stiffener:			

Z ≥ N in general; Z < N for stiffeners simply supported at both ends	$\lvert\frac{M_{SW,H}}{I_Y}(Z-N)\rvert 10^{-3}$	$\lvert\frac{0.625M_{WV,H}}{I_Y}(Z-N)\rvert 10^{-3}$	
Z < N in general; Z ≥ N for stiffeners simply supported at both ends	$\lvert\frac{M_{SW,S}}{I_Y}(Z-N)\rvert 10^{-3}$	$\lvert\frac{0.625F_D M_{WV,S}}{I_Y}(Z-N)\rvert 10^{-3}$	

The normal stress and shear stress calculated above are to be checked according to the following formulae:

$$\frac{R_y}{\gamma_R \gamma_m} \geq \sigma \tag{3.51}$$

$$0.5\frac{R_y}{\gamma_R \gamma_m} \geq \tau \tag{3.52}$$

The minimum net shear sectional area A_{Sh}, in cm^2, and the net section modulus *W*, in cm^3 for ordinary longitudinal stiffener subjected to lateral pressure are to be not less obtained from the following formulae:

$$A_{Sh} = 10.\gamma_R.\gamma_m.\beta_S.\frac{\gamma_{S2}.p_s + \gamma_{W2}.p_W}{R_y}.\left(1-\frac{S}{2.l}\right).S.l \tag{3.53}$$

$$W = \gamma_R.\gamma_m.\beta_b.\frac{\gamma_{S2}.p_s + \gamma_{W2}.p_W}{m\left(R_y - \gamma_R.\gamma_m.\sigma_{x1}\right)}.\left(1-\frac{S}{2.l}\right).S.l^2.10^3 \tag{3.54}$$

3.10 Buckling

The structural elements of the ship are subject to the following loads and their combinations: axial, bending, shear, cyclic and dynamic. One of the main failure modes of these elements is their buckling and structural instability.

The equilibrium of the structural members determines the stability of ships and marine structures. The initially designed structure differs from the actual structure due to slight imperfections, deviations and defects. The structure is stable when in the occurrence of minor defects and imperfections they cause slight deviations, and it is unstable when in the occurrence of the minor defects and imperfections they originate enormous deviations. Due to the existence of deviations, the geometry of the structure and its stanchions must be designed and selected to ensure stability in the structure and its structural elements in the face of all kinds of disturbances that may occur. The relationship between the type of disturbance and the consequences that result in it defines the concept of stability of a structure (Amdahl, 2009).

The common causes of plate buckling of ship structures are:

- High compressive residual stresses.
- High compressive stresses.
- High shear stresses.
- Combined stresses.

- Lack of flexural rigidity.
- Lack of stiffening.
- Extensive and improper use of High Tensile Steel (HTS).
- Excessive material wastage due to general and local corrosion.

The general modes of failure of stiffened panels are:

- Lateral buckling of stiffeners.
- Torsional buckling of stiffeners.
- Flexural buckling of stiffeners.
- Flexural buckling for plate stiffener combination.
- Buckling of plate panel between stiffeners.

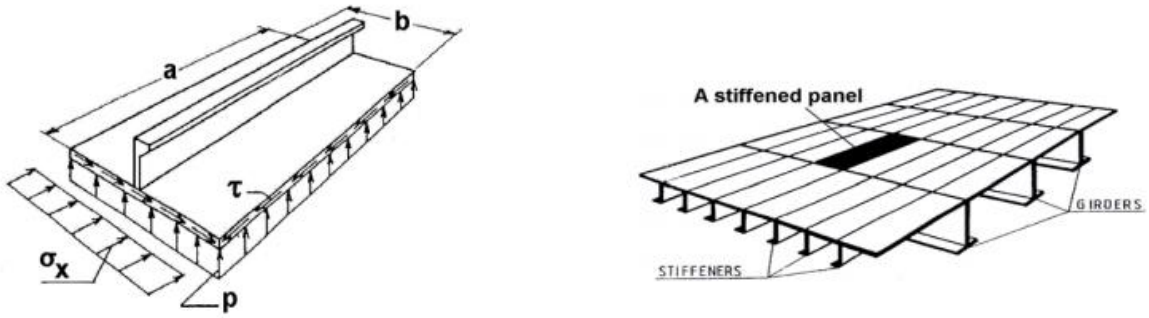

Figure 3.26 – Typical plate panel structural configuration.

3.10.1 Plating

The buckling check of plating, subjected to compression and bending along one side, with or without shear, is shown in *Figure 3.27*.

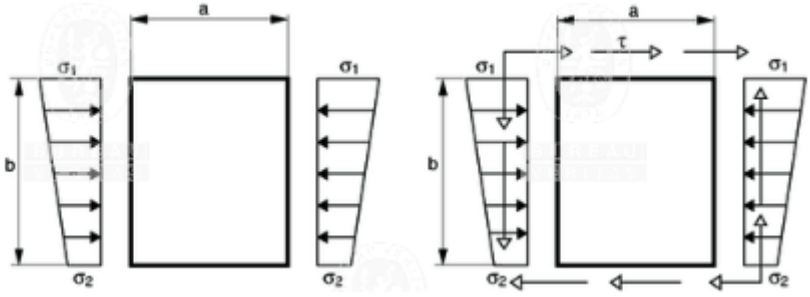

Figure 3.27 – Buckling for plate panel subjected to compression and bending, with and without shear (BV 2019 Rules).

The compression stress varies linearly from σ_1 to σ_2 along edge "*b*". The load pattern, ψ, is given as:

$$\Psi = \frac{\sigma_2}{\sigma_1} \tag{3.55}$$

The buckling factor K_1 for plate panel is given in *Table 3.24*.

Table 3.24 – Buckling factor K_1 (BV, 2019 Rules).

Load Pattern	Aspect Ratio	Buckling factor K_1
$0 \leq \psi \leq 1$	$\alpha \geq 1$	$\frac{8.4}{\Psi + 1.1}$
	$\alpha < 1$	$(\alpha + \frac{1}{\alpha})^2 . \frac{2.1}{\Psi + 1.1}$
$-1 \leq \psi \leq 0$	-	$(1+\Psi)K_1' - \Psi K_1'' + 10.\Psi(1+\Psi)$
$\Psi \leq -1$	$\alpha \frac{1-\Psi}{2} \geq \frac{2}{3}$	$23.9(\frac{1-\Psi}{2})^2$
	$\alpha \frac{1-\Psi}{2} < \frac{2}{3}$	$(15.87 + \frac{1.87}{(\alpha \frac{1-\Psi}{2})^2} + 8.6(\alpha \frac{1-\Psi}{2})^2)(\frac{1-\Psi}{2})^2$

For the buckling check of plating, the normal stresses of hull girder compression are obtained in N/mm^2, from *(3.44)*.

The hull girder normal stresses σ_{S1}, σ_{WV1}, σ_{WH1} are defined by the formulae given in *Table 3.25*.

Table 3.25 – Hull girder normal stresses σ_{S1}, σ_{WV1}, σ_{WH1} (BV, 2019 Rules).

Condition	$\sigma_{S1}\ [N/mm^2]$	$\sigma_{WV1}\ [N/mm^2]$	$\sigma_{WH1}\ [N/mm^2]$
Z ≥ N	$\frac{M_{SW,S}}{I_Y}(Z-N)10^{-3}$	$\frac{0.625F_D M_{WV,S}}{I_Y}(Z-N)10^{-3}$	$-\lvert\frac{0.625M_{WH}}{I_Z}y\rvert 10^{-3}$
Z < N	$\frac{M_{SW,H}}{I_Y}(Z-N)10^{-3}$	$\frac{0.625M_{WV,H}}{I_Y}(Z-N)10^{-3}$	

The combination factors for each load case are presented in *Table 3.17*.

The critical buckling stress for compression and bending is to be obtained in N/mm^2, from the following formulae:

$$\sigma_c = \sigma_E \; for \; \sigma_E \leq \frac{R_{eH}}{2} \tag{3.56}$$

$$\sigma_c = R_{eH}\left(1 - \frac{R_{eH}}{4\sigma_E}\right) for \; \sigma_E > \frac{R_{eH}}{2} \tag{3.57}$$

where σ_E is the Euler buckling stress in N/mm^2, given as:

$$\sigma_E = \frac{\pi^2 E}{12(1-\upsilon^2)}(\frac{t}{b})^2 K_1 \varepsilon 10^{-6} \tag{3.58}$$

$$\sigma_E = \frac{\pi^2 E}{12(1-\upsilon^2)}(\frac{t}{b})^2 K_3 10^{-6} \tag{3.59}$$

The bucking factor K_1 is for plane plate panel and K_3 is the buckling factor for curved plate panels.

So, K_3 is given as:

$$K_3 = 2\left(1+\sqrt{1+\frac{12(1-\upsilon^2)}{\pi^4}\frac{b^4}{r^2 t^2}10^6}\right) \tag{3.60}$$

The critical shear bucking stress for shear is to be obtained in *N/mm*^{2}, from the following formulae:

$$\tau_c = \tau_E \; for \;\; \tau_E \leq \frac{R_{eH}}{2\sqrt{3}} \tag{3.61}$$

$$\tau_c = \frac{R_{eH}}{\sqrt{3}}\left(1-\frac{R_{eH}}{4\sqrt{3}\tau_E}\right) for \; \tau_E > \frac{R_{eH}}{2\sqrt{3}} \tag{3.62}$$

where τ_E is the Euler shear buckling stress in *N/mm*^{2}, given as:

$$\tau_E = \frac{\pi^2 E}{12(1-\upsilon^2)}(\frac{t}{b})^2 K_i 10^{-6} \tag{3.63}$$

The buckling factor K_i present on *(3.63)*, can be the buckling factor for plane plate panel (K_2) or the bucking factor for curved plate panel (K_4) depending on the plate to be analysed.

The bucking factors K_2 and K_4 are to be taken equal to:

$$K_2 = \; 5.34 \; + \frac{4}{\alpha^2} \; for \; \alpha \; > 1 \tag{3.64}$$

$$K_2 = \frac{5.34}{\alpha^2} + 4 \; for \; \alpha \; \leq \; 1 \tag{3.65}$$

$$K_4 = \frac{12(1-\upsilon^2)}{\pi^2}\left(5+\frac{b^2}{rt}10^2\right) \tag{3.66}$$

where *α* is the aspect ratio of the panel defined as $\alpha \; = \frac{a}{b}$.

The critical buckling stress for plate panels subjected to compression and bending is to be checked with the following formula:

$$\frac{\sigma_c}{\gamma_R \gamma_m} \geq |\sigma_b| \tag{3.67}$$

The net buckling thickness, in *mm*, for compression and bending plate is to be obtained from the following formulae:

$$t = \frac{b}{\pi}\sqrt{\frac{12\gamma_R\gamma_m|\sigma_b|(1-\upsilon^2)}{EK_i\varepsilon}}10^3 \; for \; \sigma_E \leq \frac{R_{eH}}{2} \tag{3.68}$$

$$t = \frac{b}{\pi}\sqrt{\frac{3R_{eH}^2(1-\upsilon^2)}{EK_i\varepsilon(R_{eH}-\gamma_R\gamma_m|\sigma_b|)}}10^3 \; for \; \sigma_E > \frac{R_{eH}}{2} \tag{3.69}$$

The critical shear buckling stress for plate panel subjected to shear is to be checked according to the following formula:

$$\frac{\tau_c}{\gamma_R\gamma_m} \geq |\tau_b| \tag{3.70}$$

The net buckling thickness, in *mm*, for the shear plate is to be obtained from the following formulae:

$$t = \frac{b}{\pi}\sqrt{\frac{12\gamma_R\gamma_m|\tau_b|(1-\upsilon^2)}{EK_i}}10^3 \; for \; \tau_E \leq \frac{R_{eH}}{2\sqrt{3}} \tag{3.71}$$

$$t = \frac{b}{\pi}\sqrt{\frac{R_{eH}^2(1-\upsilon^2)}{EK_i\left(\frac{R_{eH}}{\sqrt{3}}-\gamma_R\gamma_m|\sigma_b|\right)}}10^3 \; for \; \tau_E > \frac{R_{eH}}{2\sqrt{3}} \tag{3.72}$$

The combined critical stress for plate panels subjected to compression, bending and shear is to be obtained from the following formulae:

$$F \leq 1 \; for \; \frac{\sigma_{comb}}{F} \leq \frac{R_{eH}}{2\gamma_R\gamma_m} \tag{3.73}$$

$$F \leq \frac{4\sigma_{comb}}{\frac{R_{eH}}{\gamma_R\gamma_m}}\left(1-\frac{\sigma_{comb}}{\frac{R_{eH}}{\gamma_R\gamma_m}}\right) for \; \frac{\sigma_{comb}}{F} > \frac{R_{eH}}{2\gamma_R\gamma_m} \tag{3.74}$$

here:

$$\sigma_{comb} = \sqrt{\sigma_1^2 + 3\tau^2} \tag{3.75}$$

$$F = \gamma_R\gamma_m\left[\frac{1+\Psi}{4}\frac{|\sigma_1|}{\sigma_E} + \sqrt{(\frac{3-\Psi}{4})^2(\frac{\sigma_1}{\sigma_E})^2 + (\frac{\tau}{\tau_E})^2}\right] \tag{3.76}$$

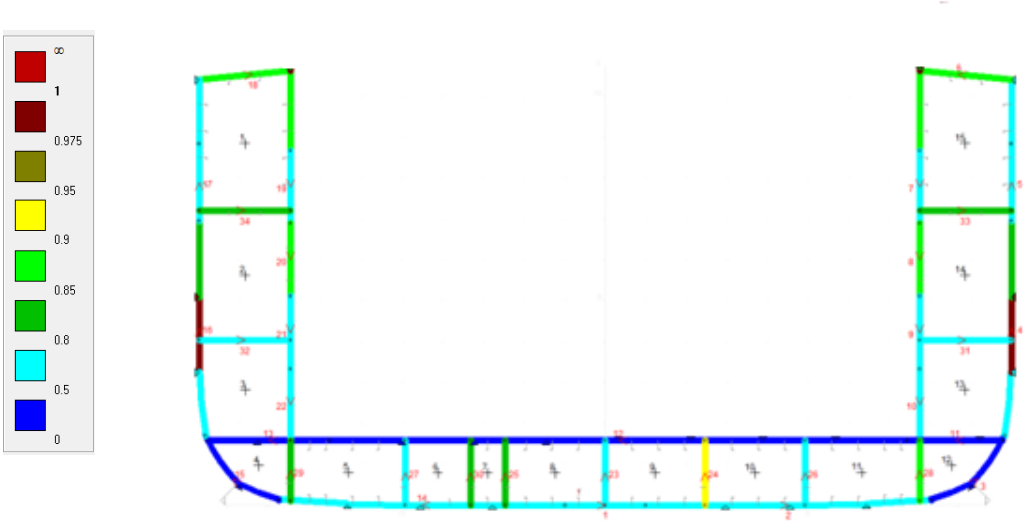

Figure 3.28 - Buckling Normal Stress for plane panel, according to the Classification Society BV, 2019.

3.10.2 Ordinary stiffeners

The critical buckling stress for compression and bending is to be obtained in N/mm^2, from the following formulae:

$$\sigma_c = \sigma_E \; for \; \sigma_E \leq \frac{R_{eH}, S}{2} \tag{3.77}$$

$$\sigma_c = R_{eH}\left(1 - \frac{R_{eH,S}}{4\sigma_E}\right) \; for \; \sigma_E > \frac{R_{eH}, S}{2} \tag{3.78}$$

where:

$$\sigma_E = Min(\sigma_{E1}, \sigma_{E2,}\sigma_{E3}) \tag{3.79}$$

The σ_{E1} is the Euler column buckling stress in N/mm^2, given as:

$$\sigma_{E1} = \pi^2 E \frac{I_e}{A_e l^2} 10^{-4} \tag{3.80}$$

where I_e is the net moment of inertia, in cm^4, and A_e is the net sectional area, in cm^2, of the stiffener width attached plating.

The σ_{E2} is the torsional column buckling stress in N/mm^2, given as:

$$\sigma_{E2} = \frac{\pi^2 E I_w}{10^4 I_p l^2}\left(\frac{K_c}{m^2} + m^2\right) + 0.385.E\frac{I_t}{I_p} \tag{3.81}$$

where:

I_w is the net sectorial moment of inertia, in cm^6, of the stiffener about its connection to the attached plating is obtained by *(3.82)* for flat bars and *(3.83)* for bulb sections:

$$I_w = \frac{h_w^3 t_w^3}{36} 10^{-6} \tag{3.82}$$

$$I_w = \frac{b_f^3 h_w^2}{12(b_f + h_w)^2} \left[t_f \left(b_f^2 + 2 b_f h_w + 4 h_w^2 \right) + 3 t_w b_f h_w \right] 10^{-6} \tag{3.83}$$

I_p is the net polar moment of inertia, in cm^4, of the stiffener about its connection to the attached plating is obtained by *(3.84)* for flat bars and *(3.85)* for stiffeners with faceplate:

$$I_p = \frac{h_w^3 t_w}{3} 10^{-4} \tag{3.84}$$

$$I_p = \left(\frac{h_w^3 t_w}{3} + h_w^2 t_f b_f \right) 10^{-4} \tag{3.85}$$

I_t is the St. Venant's net moment of inertia, in cm^4, of the stiffener without attached plating is obtained by *(3.86)* for flat bars and *(3.87)* for stiffeners with faceplate:

$$I_t = \frac{h_W t_W^3}{3} 10^{-4} \tag{3.86}$$

$$I_t = \frac{1}{3} \left(h_w t_w^3 + b_f t_f^3 \left(1 - 0.63 \frac{t_f}{b_f} \right) \right) 10^{-4} \tag{3.87}$$

m is the number of half-waves defined by:

$$m^2 (m-1)^2 \leq K_c < m^2 (m+1)^2 \tag{3.88}$$

K_c is defined by the following formula:

$$K_c = \frac{C_0 l^4}{\pi^4 E I_w} \tag{3.89}$$

C_0 is the spring stiffness of the attached plating given by:

$$C_0 = \frac{t_p^3 E}{2.73 s} 10^{-3} \tag{3.90}$$

The σ_{E3} is the Euler buckling stress of the stiffener web, in N/mm^2, given by *(3.91)* for flat bars and *(3.92)* for stiffeners with faceplate.

$$\sigma_E = 16 (\frac{t_w}{h_w})^2 10^4 \tag{3.91}$$

$$\sigma_E = 78 (\frac{t_w}{h_w})^2 10^4 \tag{3.92}$$

The critical buckling stress of the ordinary stiffeners is to be checked according to the following formula:

$$\frac{\sigma_c}{\gamma_R \gamma_m} \geq |\sigma_b| \tag{3.93}$$

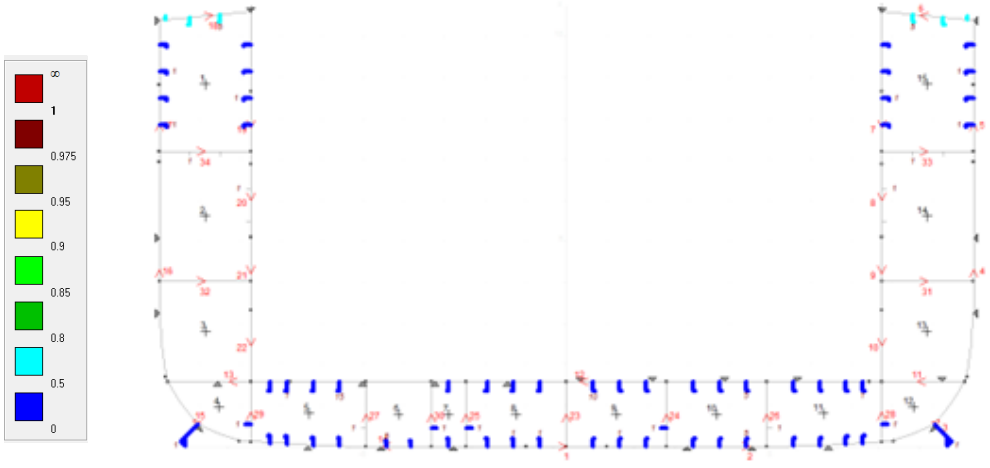

Figure 3.29 – Buckling Normal Stress for longitudinal stiffeners, according to the Classification Society BV, 2019.

3.11 Ultimate girder strength

MARS 2000 allows the study of ship strength in the plastic domain and predicts the loads that lead to its collapse. Provided by the Bureau Veritas (*BV, 2019*), the software adopts the progressive collapse method (Smith,1977) to analyse the ultimate strength of the hull girder between two adjacent frames.

The midship section of the ship is divided into two types of structure elements: stiffener attaching plating element and hard corner element, acting independently in their failure modes. The curvature momentum curve is obtained using an incremental-iterative approach. For each iteration, the bending moment acting on the hull girder transverse section increases due to the imposed curvature. Each structural member has an axial strain due to the angle of rotation of the hull girder transverse section about its horizontal neutral axis. The structural elements above the neutral axis are shortened, while the structural elements below the neutral axis are lengthened in the sagging conditions. The location of the neutral axis and the cross-section of the ship are calculated based on the failure mode of each structural element as the external moment is applied. The tensile structural elements present a single mode of elastic-plastic failure, while in compression, they present the mode of buckling or yielding (Da-wei & Gui-jie, 2018).

The ultimate strength of the structure in the analysis is present in *Figure 3.30*.

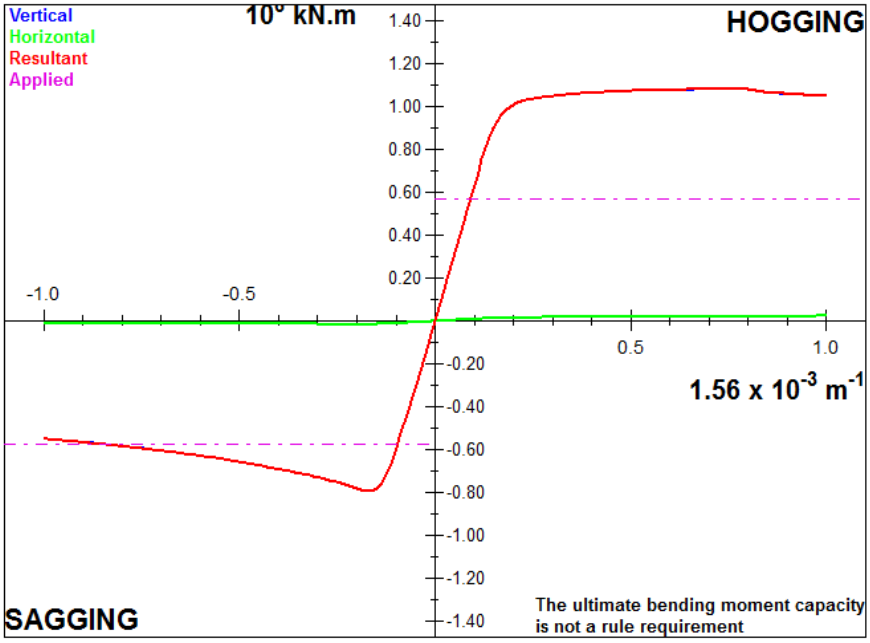

Figure 3.30 – Ultimate strength of the structure (MARS 2000 software).

The pink dashed line shows the minimum bending moment that the hull girder needs to support before it reaches the yield point (as defined by the classification society, in this case, from *BV, 2019).* It can also be observed that the higher bending moments occur in the hogging condition. As can be seen, the bending moments experienced by the structure during a cycle are higher during hogging and lower during sagging. If we consider that the critical situation occurs on the deck because it is the farthest point of the neutral axis. Considering that this critical situation occurs in compression, it is concluded that the worst possible situation for the structure occurs during sagging.

3.12 Geometric properties of midship section

The final thickness of the plate panel and the section modulus and shear area of profiles used in the midship section subjected to yielding, buckling and ultimate strength according to the Classification Society – Bureau Veritas are shown in the following figures.

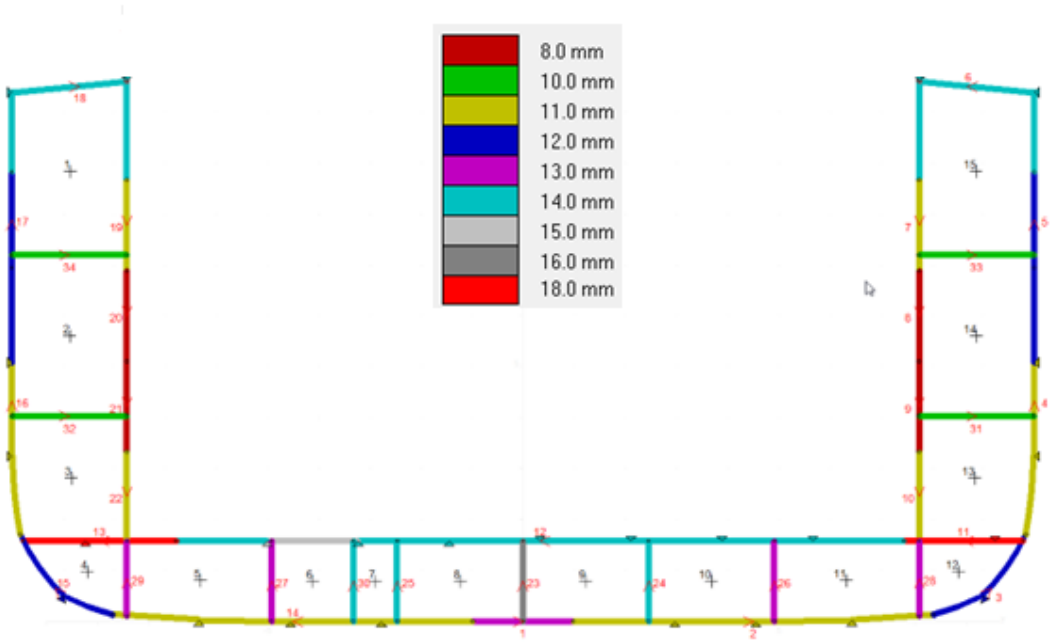

Figure 3.31 – Plate panel final thickness, according to the Rules of Classification Society BV, 2019.

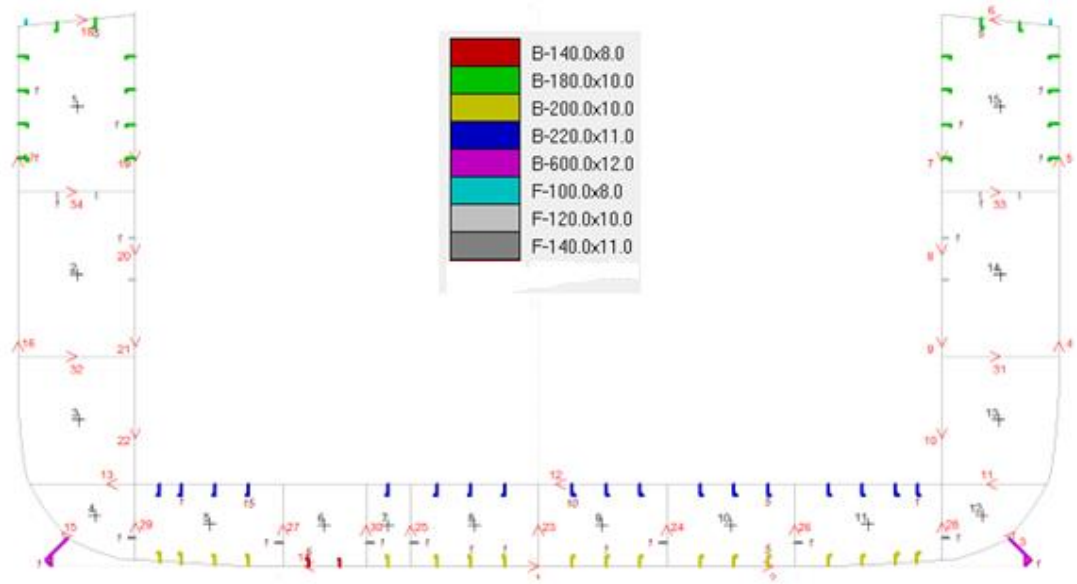

Figure 3.32 – Final longitudinal ordinary stiffeners, according to the Rules of Classification Society BV, 2019.

The geometric properties of the midship section according to the thickness of the plate panels (*Figure 3.31*) and the section modulus of the profiles (*Figure 3.32*) subject to the requirements imposed by the classification society are shown in *Table 3.26*.

Table 3.26 – Geometric properties of midship section.

$A\ [m^2]$	$N[m]$	$I_{na}[m^4]$	$I_{ZZ}[m^4]$	$Z_{deck}[m^3]$	$Z_{bottom}[m^3]$
1.55	3.87	23.47	81.96	3.59	6.06

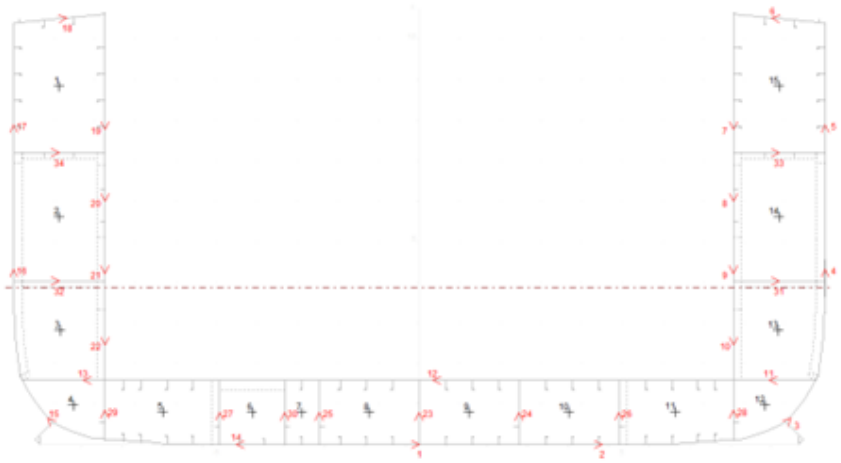

Figure 3.33 – Neutral axis position.

4. STRUCTURAL RELIABILITY ASSESSMENT

The reliability analysis of a structure or a structural element, according to Freudenthal et al. (1966), is composed of two variables: the applied load (*Z*) and the resistance of the structure (*S*) that supports it, and is carried out based on a limit state function defined as:

$$G(x) = S - Z \tag{4.1}$$

It is assumed by Melchers (1999) that only the safety of a structural element will be considered, i.e., the structural response of the element (*S*) must always be higher than the applied load (*Z*). The probability of failure, P_f of the structural element is defined by:

$$P_f = P(S \leq Z) = P(S - Z \leq 0) = P(\frac{S}{Z} \leq 1) \tag{4.2}$$

$$P_f = P[G \leq 0] \tag{4.3}$$

The cumulative distribution function (CDF) for a random variable *X* is given by:

$$F_x(x) = P(X \leq x) = \int_{-\infty}^{x} f_x(x)\, dx \tag{4.4}$$

If the resistance of the structure (*S*) and the imposed load (*Z*) are independent, the probability of failure of the structure is given by:

$$P_f = P(S - Z \leq 0) = \int_{-\infty}^{\infty} \int_{-\infty}^{s \geq z} f_S(s).f(z)\, ds\, dz = \int_{-\infty}^{\infty} F_s(z)\,.f_z(z)\, dz \tag{4.5}$$

where *f* represents the probability density function (PDF).

If the limit state function *G(x)* is linear, the random variables (*S*, *Z*) follow normal distributions of means μ_S and $\mu_Z$and variances σ_S^2 and σ_Z^2 and it is possible to solve the integral of revolution *(4.5)* (Melchers, 1999). The mean and variance are obtained by addition and subtraction, respectively, of the normal random variables *S* and *Z*. Therefore, the probability of failure is defined by (Cornell, 1969):

$$P_f = P(S - Z \leq 0) = P\,(\,G \leq 0) = \Phi\left(\frac{-(\mu_S - \mu_Z)}{(\sigma_S^2 + \sigma_Z^2)^{\frac{1}{2}}}\right) = \Phi\,(-\beta_C) \tag{4.6}$$

where Φ is the normal probability distribution function with null mean value and unit standard deviation, and β_C is the Cornell reliability index defined by:

$$\beta_C = \frac{\mu_G}{\sigma_G} \tag{4.7}$$

The method described above is valid when the limit state function is a linear function consisting of more than two random variables with normal distribution, defined by:

$$g(X) = a_0 + a_1.X_1 + a_2.X_2 + \ldots + a_n.X_n \tag{4.8}$$

where *g(x)* is a linear function that follows a normal distribution with mean and standard deviation calculated directly.

Generally, the limit state function G(x) = 0 is a nonlinear function. Proceeding to a Taylor series expansion around the maximum likelihood point (x^*) of the limit state function (Hasofer et al., 1974), it is possible to linearize G(x) = 0, considering first order methods (*FORM*).

$$\mu_G \approx g(x^*) \tag{4.9}$$

$$\sigma_G^2 \approx (\frac{\partial g}{\partial X_i})^2\, |x^*\, \sigma_{x_i}^2 \tag{4.10}$$

4.1 First order reliability method (FORM)

If the defined limit state function is a time-invariant problem, the reliability index proposed by Cornell varies if it is replaced by an equivalent one (Ditlevsen, 1973). Using the Hasofer & Lind (1974) transformation, defined by the equation *(4.11)*, it is possible to transform all the independent variables with Normal probability distribution (*PDF*) X_i into a set (*U*) of random variables, with null mean value and

unit variance (*N* (0,1)). The transformation (U_i) is only applicable if the variables are statistically independent and follow a normal distribution.

$$U_i = \frac{X_i - \mu_{X_i}}{\sigma_{X_i}} \tag{4.11}$$

In *Figure 4.1*, according to Hasofer & Lind, the reliability index (β_{HL}) is defined as the minimum distance from the origin to the limit state surface (*g(u) = 0*). In the reduced space or the normalized space, the boundary surface area (*g(u) = 0*) is linearized around the point of the boundary state surface closest to the origin of the normalized space.

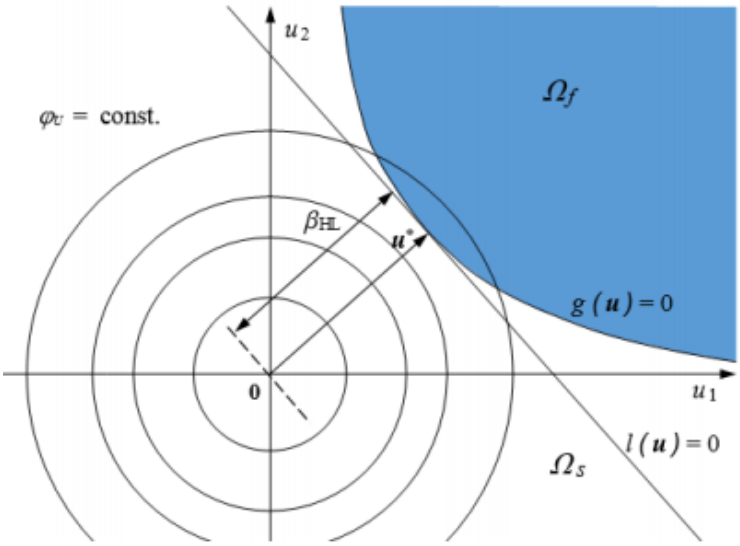

Figure 4.1 - Hasofer & Lind (1974) Index.

Using the transformation described above in *(4.11)*, the probability of failure is defined as:

$$P_f = \int_{g(x)\leq 0} f_X(x)dx = \int_{g(u)\leq 0} \varphi_u(u)du \tag{4.12}$$

where φ_u is the normal probability density function (PDF) of *U*, defined by:

$$\varphi_U = \frac{1}{(2\pi)^{n/2}} exp[-\frac{1}{2}||u||^2] \tag{4.13}$$

Due to the probability density function (φ_u) defined immediately above presenting rotational symmetry, the probability of failure proposed by Hasofer & Lind (1974) is approximated by:

$$P_f \approx \phi\,(-\beta_{HL}) \tag{4.14}$$

where (β_{HL}) is the reliability index given by:

$$\beta_{HL} = ||u^*|| \tag{4.15}$$

where (u^*) is the obtained point (see *Figure 4.1*) of the solution to the optimisation problem with the following constraints:

$$\begin{cases} minimize\ ||u|| \\ subject\ to\ g(u)\ =\ 0 \end{cases} \tag{4.16}$$

The coefficient of sensitivity (α_i) of the variable X_i is defined as:

$$\alpha_i\ =\ \frac{(\frac{\partial g}{\partial U_i})^*}{\sqrt{\sum_{i=1}^{n}(\frac{\partial g}{\partial U_i})^{*^2}}} \tag{4.17}$$

Therefore, the relation between the coordinates of the point (u^*) and (*β*) is given by:

$$\frac{U_i^*}{\beta}\ =\ \alpha_i \tag{4.18}$$

If the sensitivity coefficient (α_i) is positive, the limit state function (*g(u) = 0*) in the normalized space increases as the variable (X_i) value increases, and the reliability index is positive, increasing its safety level.

4.2 Ultimate limit state design

When a structure or a partial structural member fails to perform a function for which it was designed, this condition defines its limit state. It is considered four types of limit state (Paik & Thayamballi, 2008):

• Serviceability limit state (SLS).

• Ultimate limit state (ULS).

• Fatigue limit state (FLS).

• Accidental limit state (ALS).

The collapse of the structure due to the loss of structural stiffness and strength, related to the loss of equilibrium, attainment of the maximum capacity of the resistance by yielding, rupture or fracture and the instability resulting from the buckling or plastic collapse of plating, stiffened panels and support members, is defined as the ultimate limit state function (ULS).

In the design of the limit state of a structure, the level of safety to be attained is determined by the type of limit state to consider. Several types of limit states have different levels of safety.

Figure 4.2 represents the structural design criteria based on the ultimate limit state (ULS). Looking at the figure, we can verify that point A represents the estimate of the buckling strength of the structure from the elastic buckling strength adjusted by a simple correction of plasticity. In the past, the designs of merchant ship structures were based on this estimate (Paik & Thayamballi, 2008).

Point B represents the ultimate strength. When load level 1 is applied to the structure, it will collapse, but if loading level 2 is applied, the structure will be safe. The safety margin of the structure is evaluated against the applied loads and their strength (Paik & Thayamballi, 2008).

The structure must be designed, so that brittle fracture does not occur, allowing ductile modes of structural failure to occur. The ductile failure mode allows the structure to redistribute internal stresses so as not to occur a sudden loss in structural strength, as opposed to the brittle fracture that leads to the complete collapse of the structure.

To avoid these failure modes, in the structural design, it is necessary to respect the toughness of the material, avoid a high concentration of stresses in the structural details and the welding defects, and allow a certain plastic deformation.

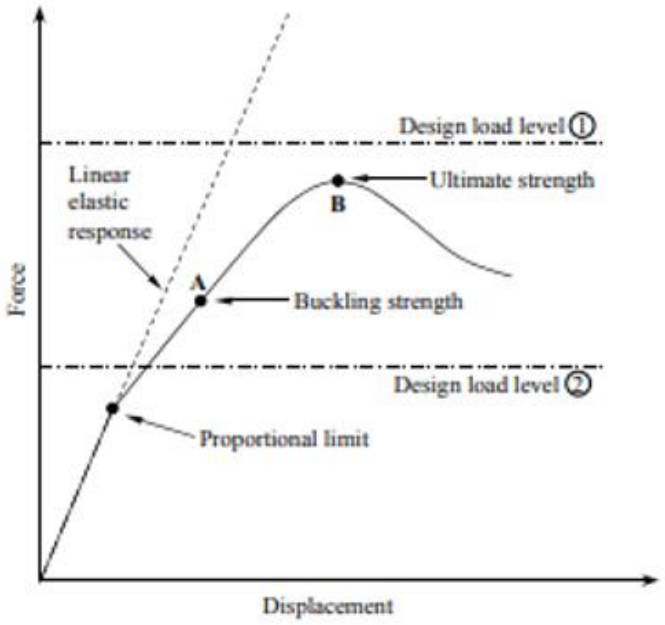

Figure 4.2 - Structural design based on the ultimate limit state (Paik & Thayamballi, 2008).

In the present study, the limit state function of the reliability assessment of the structure is based on the ultimate strength of the ship hull defined as (Guedes Soares et al., 1996):

$$g = \tilde{x}_u.\tilde{M}_u - (\tilde{x}_{sw}.\tilde{M}_{sw} - \tilde{x}_w.\tilde{x}_s.\tilde{M}_w) \tag{4.19}$$

where $\tilde{M}_u$ is the ultimate bending moment; $\tilde{M}_{sw}$ is the still water bending moment; $\tilde{M}_w$ is the wave-induced bending moment; $\tilde{x}_u$ is uncertainty model on ultimate strength; $\tilde{x}_{sw}$ is uncertainty model prediction on still water bending moment; $\tilde{x}_w$ is the error in the wave-induced bending moment due to linear seakeeping analysis and $\tilde{x}_s$ is nonlinearities in sagging.

The statistical descriptions of the uncertainty coefficients($\tilde{x}_u$, $\tilde{x}_{sw}$, $\tilde{x}_w$, $\tilde{x}_s$) involved in the limit state function (*4.19*) are assumed here as:

$$\tilde{x}_u \sim N\{1.05; 0.1\} \quad (4.20)$$

$$\tilde{x}_{sw} \sim N\{1.00; 0.1\} \quad (4.21)$$

$$\tilde{x}_w \sim N\{1.00; 0.1\} \quad (4.22)$$

$$\tilde{x}_s \sim N\{1.00; 0.1\} \quad (4.23)$$

The uncertainty coefficients ($\tilde{x}_{sw}, \tilde{x}_w, \tilde{x}_s$), are fitted to a Normal distribution of the mean value of 1.00 and standard deviation of 0.1. The model uncertainty on ultimate strength ($\tilde{x}_u$) is fitted to a Normal distribution of the mean value of 1.05 and a standard deviation of 0.1.

In calculating the reliability index of the ultimate limit state of the structure, the first order reliability method (*FORM*) is used.

The still water bending moment (M_{SW}) is fitted to a Normal distribution. According to Guedes Soares & Moan (1988) and Guedes Soares (1990), the statistical descriptors of the still water bending moment (M_{SW}) are defined by regression equations as a function of length *L* and deadweight ratio *W* of the ship.

The deadweight ratio (*W*) of the ship is defined as:

$$W = \frac{DWT}{Full\ Load} \quad (4.24)$$

So, the statistical descriptors of the still water bending moment (M_{SW}) are estimated as:

Table 4.1 – Statistical descriptors of the still water bending moment (M_{SW}).

	a_0	a_1	a_2
$Mean(M_{sw,max}) = a_0 + a_1.W + a_2.L$	114.7	-105.6	-0.154
$StDev(M_{sw,max}) = a_0 + a_1.W + a_2.L$	17.4	-7	0.035

The minus sign of $Mean(M_{sw,max})$ indicates that the maximum bending moment of the ship is in sagging.

$$Mean(M_{sw}) = \frac{Mean(M_{sw,max})M_{sw,CS}}{100} \quad (4.25)$$

$$StDev(M_{sw}) = \frac{StDev(M_{sw,max})M_{sw,CS}}{100} \quad (4.26)$$

Considering that the wave-induced bending moment (M_w) can be represented as a stationary Gaussian process. The distribution of the extreme values at a random point over a specified time is assumed to be the Gumbel distribution. The wave-induced bending moment (M_w) given by the classification society Rules (*BV, 2019*) may be modelled as a Weibull distribution with a probability of exceedance of 10^{-8}, defined as:

$$F_{M_W} = 1 - e^{(\frac{M_W}{q})^h} \tag{4.27}$$

where *q* and *h* are the statistical descriptors of the wave-induced bending moment (M_w) may be defined as:

$$q = \frac{M_{w,CS}}{ln(10^8)^{\frac{1}{h}}} \tag{4.28}$$

$$h = 2.26 - 0.54.log_{10}(L) \tag{4.29}$$

The Gumbel distribution function is described as:

$$F_{M_W} = exp\{-exp(-\frac{M_{W,e} - \alpha_m}{\beta_m})\} \tag{4.30}$$

where $M_{w,e}$ is a random variable that represents the extreme value of the vertical wave-induced moment; α_m and β_m are the parameters of the Gumbel distribution can be defined as:

$$\alpha_m = q(ln(n))^h \tag{4.31}$$

$$\beta_m = \frac{q}{h}(ln(n))^{\frac{(1-h)}{h}} \tag{4.32}$$

where *q* and *h* are the factors of the Weibull distribution function (defined in *(4.28)* and *(4.29)*, respectively); *n* is the mean number of load cycles calculated as:

$$n = \frac{p.T_r.(365).(24).(3600)}{T_w} \tag{4.33}$$

where *p* is the partial time in which the ship is in seagoing conditions; T_r is the reference time and T_w is the mean value wave period. The assumed values of *p*, T_r and T_w can be shown in *Table 4.2*.

Table 4.2 – Assumed Values of p, T_r and T_w.

p, [-]	0.4
T_r, [*year*]	1.0
T_w, [*s*]	8.0

Using the *MARS 2000* software calculates the value of the confidence level of 5% of the ultimate bending moment, $M_u^{5\%} = M_u^C$. It is fitted to a lognormal probability density function defined by equation *(4.34)*, with the variance and mean value defined by *(4.35)* and *(4.36),* respectively. It is assumed that covariance (*COV*) is equal to 0.08.

$$f_{Mu} = \frac{1}{M_u \sigma_{Mu} \sqrt{2\pi}} e^{-\frac{ln(M_u) - \mu_{Mu}}{2\sigma_{Mu}^2}} \tag{4.34}$$

$$\sigma_{Mu} = \sqrt{ln(COV^2 + 1)} \tag{4.35}$$

$$\mu_{Mu} \rightarrow F_{Mu}^{-1}(0.05, \mu_{Mu}, \sigma_{Mu}) = M_u^{5\%} \tag{4.36}$$

Based on the characteristics values of the calculated confidence levels (5%, 95%, 95%) of their original probability density functions (M_u^C, M_{sw}^C and M_w^C) and the design values of all parameters (M_u^*, M_{sw}^*, x_u^*, x_{sw}^*, x_w^* and x_s^*) involved in state functions, the partial safety factors ($\gamma_u, \gamma_{sw}, \gamma_w$) are estimated with a particular beta reliability index.

$$\gamma_u = \frac{M_u^C}{x_u^* M_u^*} \tag{4.37}$$

$$\gamma_{sw} = \frac{x_{sw}^* M_{sw}^*}{M_{sw}^C} \tag{4.38}$$

$$\gamma_w = \frac{x_s^* x_w^* M_w^*}{M_w^C} \tag{4.39}$$

The reliability index of the midship hull structure for the net and gross designs can be related assuming that at the end of the service life of the ship ($\tau_s = 25\ years$), when the structure of the ship is already corroded, i.e. there is no corrosion margin determined by the classification society rules, *BV, 2019* defined in the previous chapter, concerning net ship hull structural design and the gross structural design is considered when non-corroded ship structure up to the moment when the corrosion protection fails. It is analysed that the structure of the midship section is subject to general corrosion, where its degradation occurs for all structural elements over the years.

Garbatov et al. (2007) defined the mean value [$d^{cd}(t)$] and standard deviation St Dev [$d^{cd}(t)$] of the corrosion depth as a function of time as:

$$Mean\ value\ [d^{cd}(t)] = d_\infty [1 - e^{(-\frac{(t-\tau_c)}{\tau_t}}], t > \tau_c \tag{4.40}$$

$$St\ Dev\ [d^{cd}(t)] = a \ln(t - \tau_c - b) - C], t < \tau_c \tag{4.41}$$

where a, b and c are coefficients.

Guedes Soares & Garbatov (1999) developed the time-dependent non-linear corrosion degradation model and the time-variant reliability index ($\beta(t)$), where $t \in [0, \tau_S]$ is defined as:

$$\beta(t) = \beta_{gross} - (\beta_{gross} - \beta_{net}) \times (1 - e^{-\frac{t-\tau_c}{\tau_t}}), t > \tau_c \tag{4.42}$$

$$\beta(t) = \beta_{gross}, t < \tau_c \tag{4.43}$$

where τ_c = *6.50 years* is the coating life and τ_t = *11 years* is the transition life.

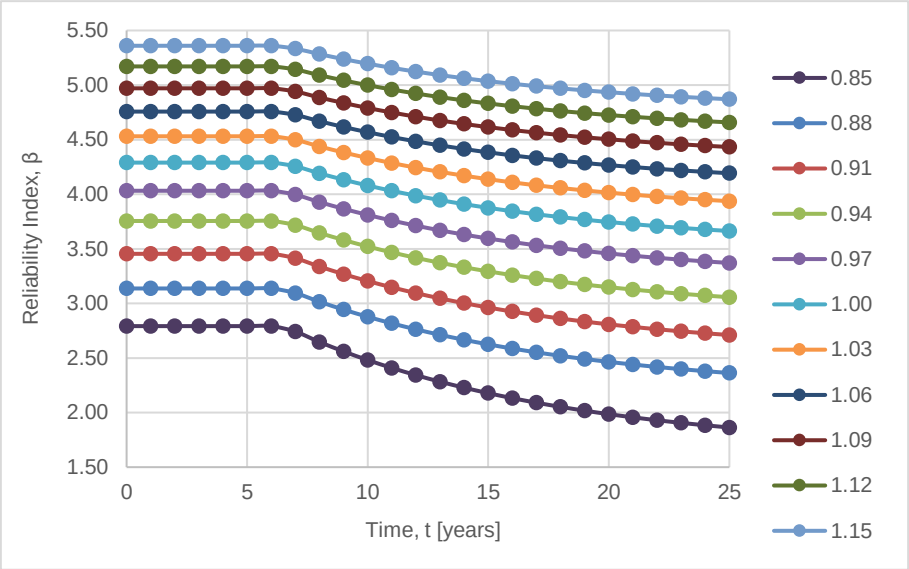

Figure 4.3 - Time variant reliability index $\beta(t)$, corrosion degradation model for design modification factor (DMF).

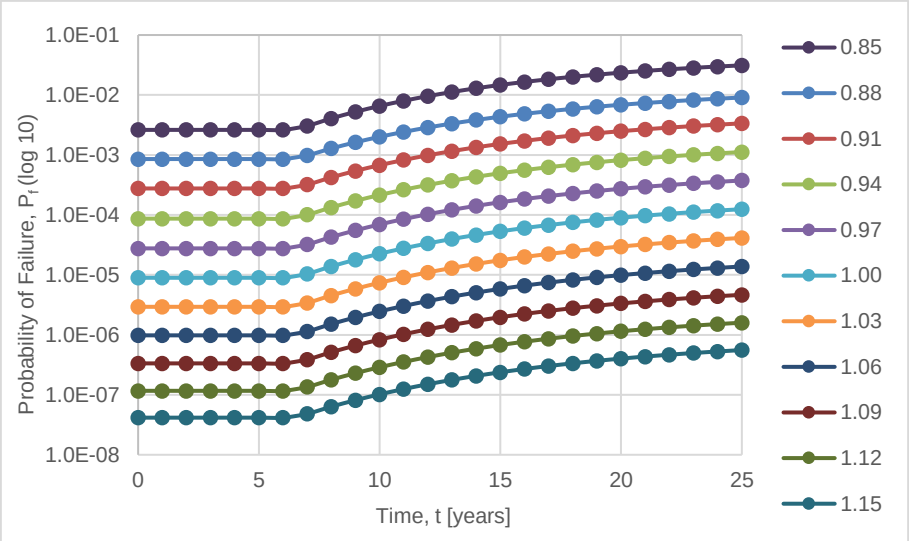

Figure 4.4 – Time variant probability of failure $P_f(log\ 10)\ (t)$, corrosion degradation model for design modification factor (DMF).

The design modification factor (*DMF*) (Guia, J. et al., 2018) represents the modification of the midship section structure, keeping the structure closest to the neutral axis constant (inner side and side shell) by changing the structure farthest from the neutral axis (bottom, double bottom and deck structure). The midship structure was modified by increasing and decreasing the thickness of the plate panel in equal measure, keeping the spacing, number and type of stiffeners constant. The *DMF* was calculated by the ratio of the modified and original midship section area (see *Table 4.3*).

Table 4.3 – Design Modification Factor (DMF) corresponding to the modification of the midship structure.

Thickness Variation [mm]	*Net area of cross section [m^2]*	*DMF*	*Gross area of cross section [m^2]*	*DMF*
-5	1.08	0.81	1.32	0.85
-4	1.15	0.86	1.36	0.88
-3	1.19	0.89	1.40	0.91
-2	1.24	0.93	1.46	0.94
-1	1.29	0.97	1.50	0.97
0	1.33	1.00	1.55	1.00
+1	1.38	1.03	1.59	1.03
+2	1.42	1.07	1.64	1.06
+3	1.47	1.10	1.68	1.09
+4	1.51	1.14	1.73	1.12
+5	1.56	1.17	1.78	1.15

The reliability index (β) and probability of failure (P_f) of intact/gross scantlings and corroded/net scantlings according to the design modification factor (DMF), shown in *Table 4.4*, *Figure 4.5* and *Figure 4.6,* based on the ultimate strength of ship hull defined on *Chapter 4.2*, in the reliability assessment of the midship structure.

Table 4.4 – Reliability index and probability of failure for design modification factor (DMF) of intact and corroded scantlings.

Intact Scantlings (Gross Scantlings)			*Corroded Scantlings (Net Scantlings)*		
DMF	β	P_f	DMF	β	P_f
0.85	2.79	2.619E-03	0.81	1.65	4.934E-02
0.88	3.14	8.544E-04	0.86	2.19	1.442E-02
0.91	3.45	2.760E-04	0.89	2.54	5.538E-03
0.94	3.76	8.664E-05	0.93	2.90	1.882E-03
0.97	4.03	2.727E-05	0.97	3.22	6.421E-04
1.00	4.29	8.942E-06	1.00	3.52	2.158E-04
1.03	4.53	2.936E-06	1.03	3.80	7.216E-05
1.06	4.76	9.812E-07	1.07	4.06	2.418E-05
1.09	4.97	3.342E-07	1.10	4.31	8.167E-06
1.12	5.17	1.166E-07	1.14	4.54	2.800E-06
1.15	5.36	4.162E-08	1.17	4.76	9.766E-07

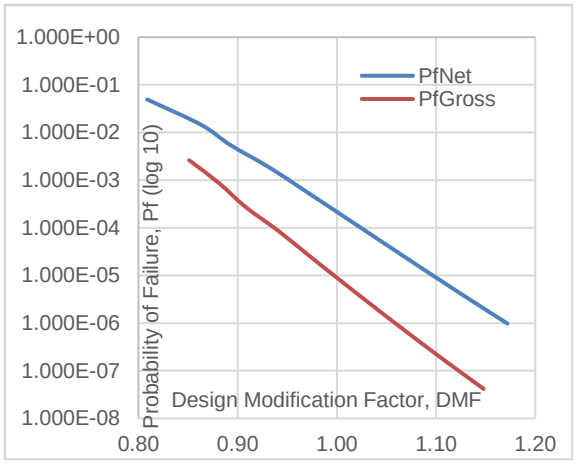

Figure 4.5 - Probability of failure P_f (log 10) for net and gross scantling according to the modification factor (DMF).

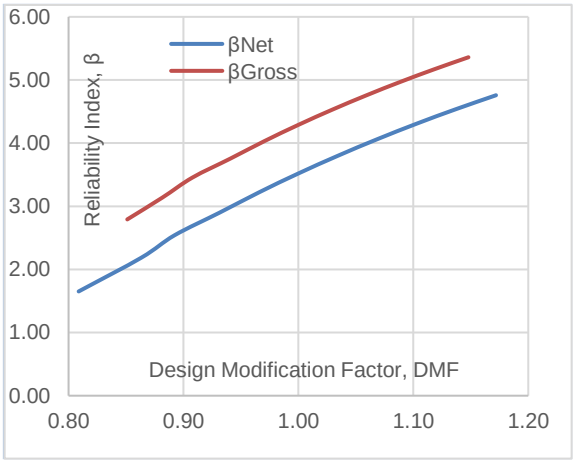

Figure 4.6 - Reliability index (β) for net and gross scantling according to the modification factor (DMF).

The sensitivity (M_w; M_u; M_{sw}; X_u; X_{sw}; X_s; X_w) and partial safety (gM_w; gM_{sw}; gM_u) factors of the structure according to the variation of design modification factors for intact/gross scantlings are shown in *Figure* 4.7 and *Figure 4.8* and for design modification factors for corroded/net scantlings are shown in *Figure* 4.9 and *Figure 4.10* respectively.

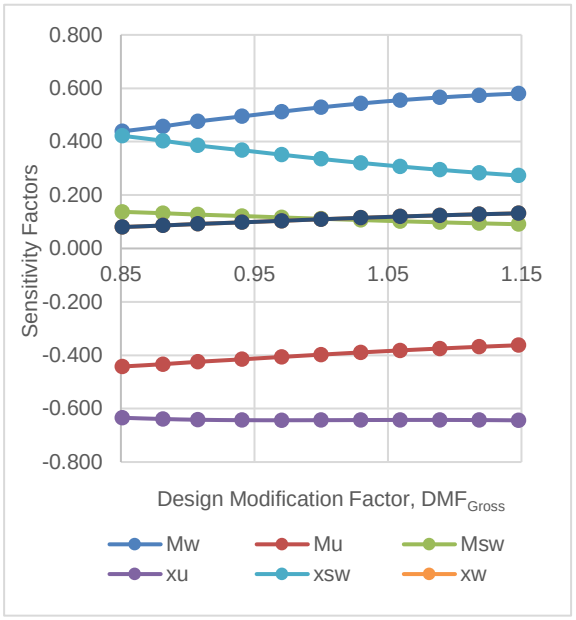

Figure 4.7 - Sensitivity factors for gross design modification (DMF_{Gross}).

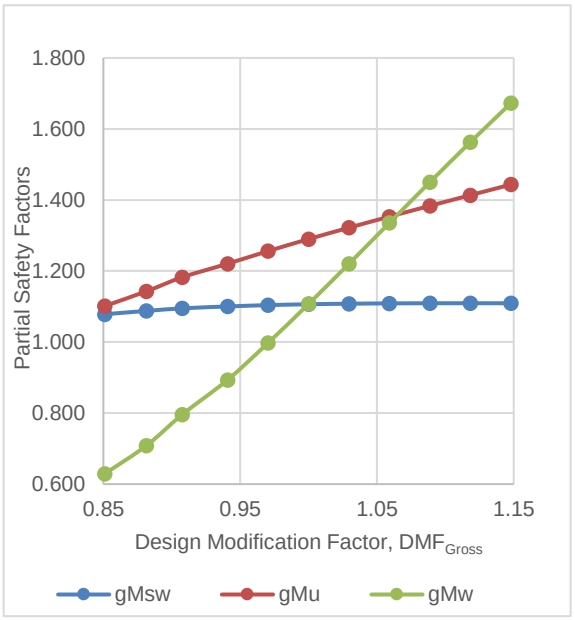

Figure 4.8 - Partial safety factors for gross design modification factor (DMF_{Gross}).

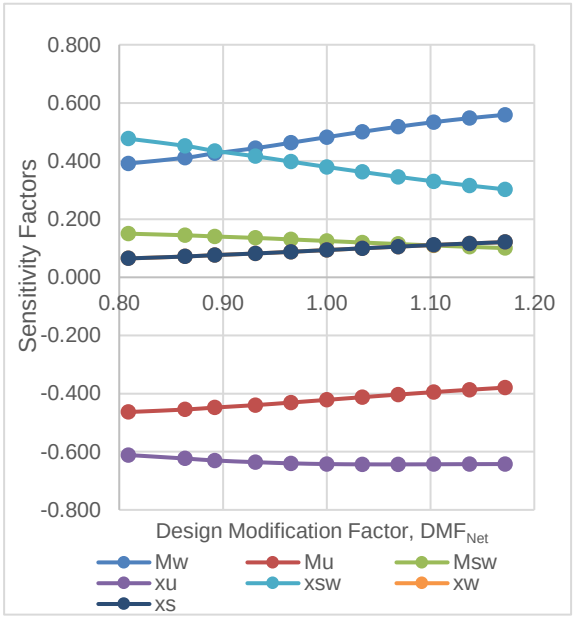

Figure 4.9 - Sensitivity factors for net design modification (DMF_{Net}).

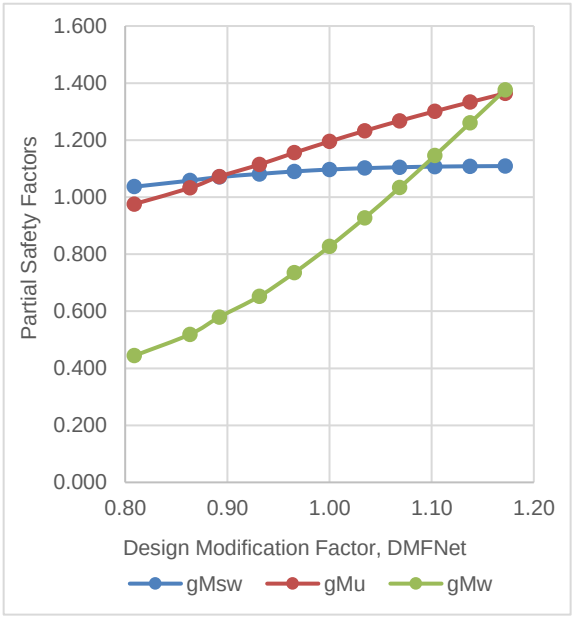

Figure 4.10 - Partial safety factors for net design modification factor (DMF_{Net}).

The results obtained in the reliability analysis of the midship section structure as a function of the design modification factor (DMF) are expected. The increase in the design modification factor (DMF), and consequently the increase in the thickness of the plate panels of the critical zones, reduces the probability of failure of the structure, i.e., it becomes more resistant subject to hull girder loads.

5. INVESTMENT COST ESTIMATION

The Life Cycle Cost (LCC) of the ship is defined as the total cost of all the different phases of life of the ship and its equipment: conception, design, acquisition, operation, maintenance, upgrade and decommissioning. It is determined by the sum of cost estimates from the beginning to the end of their life cycle. It is usually used in the design process of all engineering systems, including ships (Damyanliev et al., 2017, Garbatov and Georgiev, 2017, Garbatov et al., 2017) and offshore structures (Yeter et al., 2016a, Yeter et al., 2016b, Yeter et al., 2017).

The costs related to the different phases of the ship's life cycle are divided into three different groups: capital costs (CAPEX), operational cost (OPEX) and decommissioning cost (DECEX).

Using predictive methods where no historical data are available and methods based on statistical data for different types of existing ships, the discount and escalation rate are introduced in the calculation of the cost of the ship to compare the current cost with the future cost that the ship may have.

Depending on sound economic decisions and the application of good engineering practices to achieve the success of any business, the ship's Life Cycle Cost Analysis (LCC) acts as a data-based decision-making tool that provides cost information considering several factors. However, the life cycle cost (LCC) of the ship provides an estimate of the cost and not an exact value of the cost of the ship, and its accuracy depends on the method used for the respective calculations and the correction of the data provided.

The present study uses the production information from five consecutively constructed multiple-purpose vessels to determine the cost estimate of the ship (CAPEX), which needs to be defined as part of an optimised ship.

5.1 Lightship estimation

The lightship weight is defined by the weight of the hull structure, deck equipment and machinery, loading and handling devices, navigation equipment, electrical equipment, furniture and fittings, main and auxiliary engine, pipelines, engine spares and liquids in machinery. In the initial stage of the project, the lightship weight is subdivided into three components: hull structure weight, equipment and outfitting weight and machinery weight.

The initial estimate of the structural weight of the vessel can be obtained by regression equations based on a statistical analysis of existing vessels (Benford, 1967, Cudina et al., 2010).

In this study, the regression equations used for estimating the lightship weight calculation are developed by Damyanliev (2001, 2002) and used in a concept project (Damyanliev et al., 2017). The recalibrated equations are based on the actual data of five multipurpose ships of similar dimensions, recently built.

The following regression equations used to estimate the lightship weight are as a function of its main characteristics: length between perpendiculars (*L*); breadth (*B*); Draught (*T*); Depth (*D*); block coefficient (*Cb*), speed (*Vs*), propulsive power (*Pw*), number of crew members (*NE*) and number of superstructure decks (*NJ*). The main characteristics of the vessel are shown in *Table 3.1*.

The weight of the ship structure in *tonnes* is defined as:

$$W_1 = (W_{11} + W_{12} + W_{13} + W_{14} + W_{15}) \tag{5.1}$$

where W_{11} is the weight of the main hull in *tonnes:*

$$W_{11} = 0.00072.C_B^{\frac{1}{3}}.L^{2.5}.\frac{T}{D}.B \tag{5.2}$$

where W_{12} is the weight of bulkheads in the main hull in *tonnes*:

$$W_{12} = 0.011.L.B.D \tag{5.3}$$

where W_{13} is the weight of decks and platforms in *tonnes*:

$$W_{13} = 0.0198.L.B.D \tag{5.4}$$

where W_{14} is the weight of the superstructure in *tonnes*:

$$W_{14} = 0.0388.L.B.NJ \tag{5.5}$$

where W_{15} is the weight of the foundation and others in *tonnes*:

$$W_{15} = 0.00275.L.B.D \tag{5.6}$$

The weight of ship equipment in *tonnes* is defined as:

$$W_2 = W_{21} + W_{22} + W_{23} + W_{24} + W_{25} + W_{26} + W_{27} + W_{28} \tag{5.7}$$

where *NCo* and *NC* are defined as:

$$NC_o = (L.B.T)^{\frac{2}{3}} + 2.B.[D - T + (NJ - 1).2.8] \tag{5.8}$$

$$NC = NC_o + 0.1.[D - T + 0.588.(NJ - 1)].L \tag{5.9}$$

where W_{21} is the weight of the anchor equipment in *tonnes*:

$$W_{21} = 0.0475.NC \tag{5.10}$$

where W_{22} is the weight of the mooring and towing arrangements in *tonnes*:

$$W_{22} = 0.0216.NC \tag{5.11}$$

where W_{23} is the weight of rudder equipment in *tonnes*:

$$W_{23} = 0.0001185.L.T.\sqrt{V_S} \quad (5.12)$$

where W_{241} is the weight of the loading equipment in *tonnes*:

$$W_{241} = 0.00883.L.B.D \quad (5.13)$$

where W_{24} is the weight of the anchor equipment and mast in *tonnes*:

$$W_{24} = W_{241} + 0.002029.L.B.D \quad (5.14)$$

where W_{25} is the weight of the outfit in *tonnes*:

$$W_{25} = 0.002325.(L.B.D) \quad (5.15)$$

where W_{26} is the weight of the hatch covers in *t*onnes:

$$W_{26} = 0.116.(L.B) \quad (5.16)$$

where W_{27} is the weight of a lifeboat and other arrangements in *t*onnes:

$$W_{27} = 0.871.NE \quad (5.17)$$

where W_{28} is the weight of other equipment in *tonnes*:

$$W_{28} = 0.0000845.L.B.D \quad (5.18)$$

The weight of the accommodation in *tonnes* are defined as:

$$W_3 = W_{31} + W_{32} + W_{33} + W_{34} + W_{35} + W_{36} \quad (5.19)$$

where M_1 and M_2 are defined as:

$$M_1 = \frac{L.B.D}{1000} \quad (5.20)$$

$$M_2 = \frac{0.22.L.B.NJ}{100} \quad (5.21)$$

where W_{31} is the weight of other equipment in *tonnes*:

$$W_{31} = 1.0182.M_2 \quad (5.22)$$

where W_{32} is the weight of the stories accommodations in *tonnes*:

$$W_{32} = 0.3854.M_1 \quad (5.23)$$

where W_{33} is the weight of the office accommodation in *tonnes*:

$$W_{33} = 0.3504.M_2 \quad (5.24)$$

where W_{34} is the weight of the painting in *tonnes*:

$$\mathrm{W}_{34} = 0.8030.\mathrm{M}_1 \tag{5.25}$$

where W_{35} is the weight of other's accommodations in *tonnes*:

$$W_{35} = 2.3772.M_1 \tag{5.26}$$

where W_{36} is the weight of isolation and others in *tonnes*:

$$W_{36} = 5.782.M_1 \tag{5.27}$$

The weight of the propulsion machinery in *tonnes* is estimated as:

$$W_4 = W_{41} + W_{42} + W_{43} + W_{44} + W_{45} + W_{46} + W_{47} \tag{5.28}$$

where W_{41} is the weight of the boilers in *tonnes*:

$$W_{41} = 0.00017.P_W \tag{5.29}$$

where W_{42} is the weight of the main engine in *tonnes*:

$$W_{42} = 0.0657.P_W \tag{5.30}$$

where W_{43} is the weight of the auxiliary machinery in ER (Engine Room) in *tonnes*:

$$W_{43} = 0.017066.P_W \tag{5.31}$$

where W_{44} is the weight of the control systems in ER, in *tonnes*:

$$W_{44} = 0.000666.P_W \tag{5.32}$$

where W_{45} is the weight of the systems and pipes in ER, in *tonnes*:

$$W_{45} = 0.0002666.P_W \tag{5.33}$$

where W_{46} is the weight of the pipes and other equipment in *tonnes*:

$$W_{46} = 0.0002666.P_W \tag{5.34}$$

where W_{47} is the weight of the other equipment in ER, in *tonnes*:

$$W_{47} = 0.0105.P_W \tag{5.35}$$

The weight of the ship's systems, in *tonnes,* is estimated as:

$$W_5 = W_{51} + W_{52} + W_{53} + W_{54} + W_{55} + W_{56} \tag{5.36}$$

where W_{51} is the weight of the hull's systems in *tonnes*:

$$W_{51} = 1.0761.M_1 \quad (5.37)$$

where W_{52} is the weight of the fire protection system in *tonnes*:

$$W_{52} = 1.2528.M_1 \quad (5.38)$$

where W_{53} is the weight of the sanitary systems in *tonnes*:

$$W_{53} = 0.8031.M_1 \quad (5.39)$$

where W_{54} is the weight of the ventilation systems in *tonnes*:

$$W_{54} = 1.4134.M_1 \quad (5.40)$$

where W_{55} is the weight of other hull systems in *tonnes*:

$$W_{55} = 0.8031.M_1 \quad (5.41)$$

where W_{56} is the weight of the other systems in *tonnes*:

$$W_{56} = 0.0964.M_1 \quad (5.42)$$

The weight of electrical equipment and control system, in *tonnes*, is defined as:

$$\mathrm{W}_6 = 3.276.\mathrm{M}_1 \quad (5.43)$$

The weight of the general ship equipment and arrangement, in *tonnes*, are defined as:

$$W_7 = PI + PTT + W_{71} \quad (5.44)$$

where PI is the weight of inventory in *tonnes*:

$$PI = 0.759.M_1 \quad (5.45)$$

where PTT is the weight of the residue liquid in ship's systems in *tonnes*:

$$PTT = 0.85.M_1 \quad (5.46)$$

where W_{71} is the weight of reserve displacement in *tonnes*:

$$W_{71} = 5.M_1 \quad (5.47)$$

Finally, the weight of the lightship, in *tonnes*, is estimated as:

$$LW = W_1 + W_2 + W_3 + W_4 + W_5 + W_6 + W_7 \quad (5.48)$$

In calculating the lightship, the welding weight was added, i.e., 2% of the total weight.

5.2 CAPEX (Capital Expenditure) estimation

In the evaluation analysis of the estimate of shipbuilding cost, the MARAD system (Maritime Administration, used by the U.S.A administration) is used to subdivide group-specific ship systems and their associated costs. The systems groups are based on the different components in the construction of the ship's life cycle, and their costs are included in the construction project. It is common to divide the ship into three different groups: W_A is the weight of the ship structure, W_B is the weight of equipment and outfitting and W_C is the weight of the propulsion machinery system.

$$W_A = W_1 \tag{5.49}$$

$$W_B = W_2 + W_3 + W_5 + W_6 + W_7 \tag{5.50}$$

$$W_C = W_4 \tag{5.51}$$

where W_1 is the weight of the ship structure, W_2 is the weight of ship equipment, W_3 is the weight of accommodation, W_4 is the weight of the propulsion machinery, W_5 is the weight of the ship's systems, W_6 is the weight of electrical equipment and control system, and W_7 is the weight of general ship equipment and arrangement.

The initial capital cost estimate CAPEX (Capital Expenditure) for constructing multi-purpose ships is based on several design parameters such as main dimensions, deadweight tonnage (DWT), weight, propulsive power, etc. By a regressions analysis, it is possible to estimate the CAPEX using a mathematical relationship between the input parameters (L, B, D, C_b, P_W, etc.) and construction cost (Garbatov et al., 2017). Construction costs are divided into material, labour, overheads and profits.

Costs related to the material include all purchases made by the shipyard: building materials, equipment and outfitting and other engineering services. The costs shown in *Figure 5.1*, the steel price variation according to (Steelbenchmark, 2019), cover different types of steel used in the construction of the ship, including its transport, profiles, castings, forgings, and welding rods.

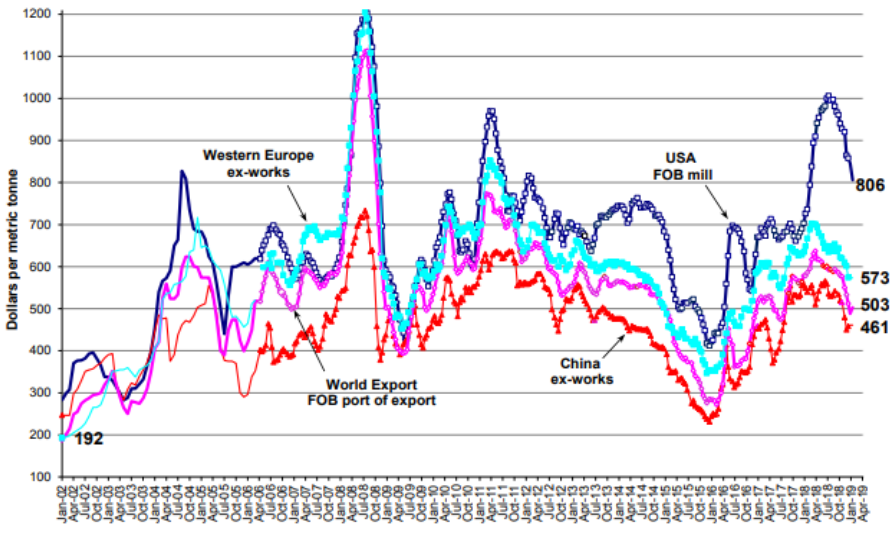

Figure 5.1 – Cost of ton steel (Steelbenchmark, 2019).

The values assumed for the price of steel and equipment are given in *Table 5.1*.

Table 5.1 – Assumed values for steel and equipment price.

k_A,[€/ton]	580
k_B,[€/ton]	1 500

Costs related to labour include wages and benefits paid to employees of the shipbuilding yard. The costs of outsourced work to companies outside the shipyard should be included in this item, the smaller shipyards having a considerable amount of subcontracted work. *Figure 5.2* shows the estimated hourly labour cost of different European countries based on Eurostat (2018). The present study assumes that the estimated hourly labour cost is 10 € / hour.

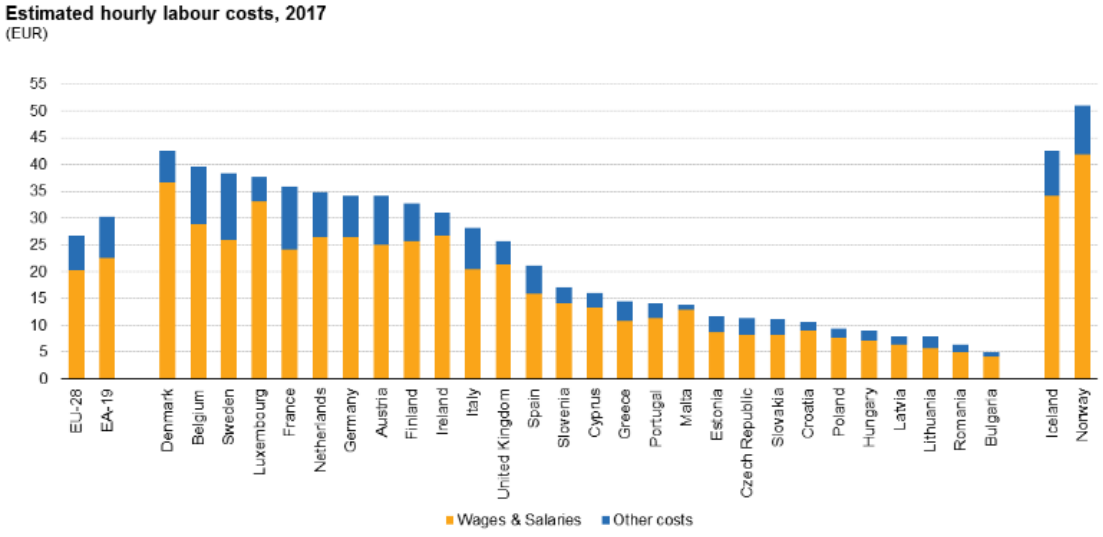

Figure 5.2 – Estimated hourly labour costs for the whole economy in euros, 2017 (Eurostat, 2018).

“Overhead costs are residual costs that cover everything that is not treated as direct cost (material and labour costs). These costs are associated with the ownership and operation of the shipbuilding yard and the non-wage costs of the skilled workforce” (Rogal et al. 2016). These costs (indirect costs) are influenced by two main factors: shipbuilding's economy and workload (in terms of Man-hours). Assumes an overhead, *O*, of the order of 25%.

The profit of the shipyard, P_R is determined by a small percentage of all the costs required to build a ship, i.e., the sum of material, labour and overhead costs. Assumes a profit of the order of 5%.

The hull structure material costs, in €, may be estimated as:

$$C_A = k_A . W_A \tag{5.52}$$

The labour cost of the hull, in *man-hours*, can be estimated as:

$$MH_A = \frac{W_A^{0.281} . L^{1.377} . B^{1.412}}{D^{0.274} . C_B^{0.487} . i^{0.102}} \tag{5.53}$$

where *i* is the series number of the ship (in this study, it is considered *i* = 1).

and the cost of the man-hour of the hull, in €, is estimated as:

$$C_{mA} = MH_A . h_{LC} \tag{5.54}$$

The material costs of the equipment and outfitting may be estimated as:

$$C_B = k_B . W_B \tag{5.55}$$

The labour cost of the equipment and outfitting, in *man-hours*, are calculated based on:

$$MH_B = \frac{W_B^{0.287} . L^{1.377} . B^{1.452}}{D^{0.272} . C_B^{0.488} . i^{0.137}} \tag{5.56}$$

and the cost of the man-hours of the equipment and outfitting is estimated as:

$$C_{mB} = MH_B . h_{LC} \tag{5.57}$$

The material costs of the propulsion machinery system may be estimated as:

$$C_C = 850\,000 . (\frac{P_W}{1000})^{0.7} \tag{5.58}$$

The labour cost of the installation of the propulsion machinery system, in man-hours, are calculated based on the newly developed regression equation:

$$MH_C = \frac{W_C^{0.292} . L^{1.224} . B^{1.417}}{D^{0.267} . C_B^{0.490} . i^{0.138}} \tag{5.59}$$

and the cost of the man-hours of the installation of the propulsion machinery system is estimated as:

$$C_{mC} = MH_C . h_{LC} \tag{5.60}$$

Finally, the CAPEX (Capital Expenditure) costs, in €, is estimated as:

$$CAPEX = [1 + P_R] \times [1 + O] \times [\sum (W_i \times C_i) + C_C + \sum C_{mi}] \tag{5.61}$$

where *i* = A is for the hull, *i* = B is for the equipment and outfitting, i = C is for the machinery, P_R is the profit, and *O* is the overhead costs.

6. COST-BENEFIT ANALYSIS

During the service life of a ship, its structure is subject to corrosion degradation, occurring structural failures due to the progressive structural collapse of the ship's hull.

To control the risk associated with the structural collapse of the ship's hull, accounting for its uncertainties based on an identified failure scenario, which may occur during its service life, risk analysis is measured as the product of the likelihood of structural failure and its consequences.

$$Risk\ (t)\ =\ \sum_j P_{f,j}\ (P[g(X_{1,j}|t) \leq 0])\ C_{f,j}(X_{2,j}|t) \tag{6.1}$$

where $P_{f,j}(P[g(X_{1,j}|t) \leq 0])$ is the probability of the failure, $C_{f,j}(X_2|t)$ is the consequence of the cost of failure, X_1 and X_2 are the vectors of parameters involved in the probability of failure and consequence analyses that occur during the service life of the ship($t \in [0,\tau_S]$).

By comparing the costs and risk associated with structural failure, the cost-benefit analysis determines when the cost to control the risk is equal to the cost of the risk due to the structural collapse of the ship's hull, thus finding the optimal value of the risk (Garbatov et al., 2018).

Risk management aims to reduce the risk to an acceptable level, by optimising the purpose and functionality of the ship's hull structural system design and evaluating alternative options for decision making.

The method used to define the level of acceptable risk is through the target reliability level that minimises the total cost of the consequence of the design of the structural system, where the various failure modes result in economic, environmental, human losses and other consequences.

The cost-benefit analysis is defined as (Garbatov et al., 2018):

$$C_{total}\ (t^n|DMF,\beta)\ =\ C_{Pf}\ (t^n|DMF,\beta) + C_{me}(DMF,\beta) \tag{6.2}$$

where $C_{Pf}\ (t^n|DMF,\beta)$ is the cost associated with the structural failure over the service life (τ_S) of the ship, estimated as a function of design modification factor (*DMF*), reliability index (β) and time (t_j), defined in *subchapter 6.1*, $C_{me}(DMF,\beta)$ is the cost of implementing a structural safety measure accounts for the design modification factor (*DMF*), which is also associated with the reliability level (β), including the cost of material and labour, that is, the redesign of the midship section hull structure, defined in *subchapter 6.2*.

6.1 Cost associated with the structural failure

The cost associated with the structural failure over the service life (τ_S) of the ship is estimated as a function of design modification factor (*DMF*), reliability index (β) and time (t_j) as (Garbatov et al., 2018):

$$C_{pf}(t^n|DMF\ ,\beta)\ =\ \sum_j^n P_f\ (t_j|DMF,\beta) \times [C_S(t_j|DMF,\beta) + C_C + C_d + C_v]e^{-\gamma t_j} \tag{6.3}$$

where $P_f(t_j|DMF,\beta)$ is the probability of failure, $C_S(t_j|DMF,\beta)$ is the cost of the ship in the year $t_j \in [0,\tau_S]$, C_C is the cost associated with the loss of the cargo, C_d is the cost associated with the accidental spill, C_v is the cost associated with the loss of human life, and γ = 5% is the assumed value of the discount rate.

The cost of the ship, $C_S(t_j|DMF,\beta)$, in €, at any time t_j is a function of the ship's age, that is, the initial cost of the ship ($t_0 = 0\ years$) and the scrapping cost($t_n = 25\ years$) accounting for corrosion degradation (Guedes Soares and Garbatov, 1999) defined in previous chapters, estimated as (Garbatov, et al., 2018):

$$C_s(t_j|DMF,\beta)\ =\ C_s(t_0|DMF,\beta) - [C_s(t_0|DMF,\beta) - C_s(t_n|DMF,\beta)] \times [1 - e^{-\frac{t_j-\tau_C}{\tau_t}}], t_j > \tau_C \tag{6.4}$$

$$C_s(t_j|DMF,\beta)\ =\ C_s(t_0|DMF,\beta), t_j\ < \tau_C \tag{6.5}$$

where $C_s(t_0|DMF,\beta)$ is the initial cost of the ship, $C_s(t_n|DMF,\beta)$ is the scrapping cost, t_j is the year of the operation [$t_j \in 0,\tau_S$], τ_s = 25 years is the service life of the ship, $\tau_C = 6.5$ years is the coating life and $\tau_t = 11$ years is the transition life.

The initial cost of the ship $C_s(t_0|DMF,\beta)$ is based on the capital cost (*CAPEX*) estimate defined in subchapter *5.2*. The scrapping cost $C_n(t_n|DMF,\beta)$ of the ship, at $t_j\ =\ t_n\ =\ 25\ years$ is estimated as (Garbatov et al, 2018):

$$C_n(t_n|DMF,\beta)\ =\ LW(t_n|DMF,\beta) \times C_{scrap} \tag{6.6}$$

where $LW(t_n|DMF,\beta)$ is the lightweight of the ship in the year ($t_j\ =\ t_n\ =\ 25\ years$) it occurs during the resale or scrap and C_{scrap} = 270 €/ton is the assumed value of scrap cost.

The lightweight of the ship in the year ($t_j\ =\ t_n\ =\ 25\ years$) is estimated to account for a design modification factor (DMF) and corrosion variation.

$$LW(t_n|DMF,\beta)\ =\ LW(t_0|DMF,\beta) \times (\delta_{corrosion}) \tag{6.7}$$

where $LW(t_0|DMF,\beta)$ is the initial lightship weight ($t\ =\ t_0\ = 0$) estimated in subchapter *5.1* and $\delta_{corrosion}$ is the corrosion variation.

Assuming in a very optimistic perspective that at the end of the ship's service life, the structural element (scantlings) does not contain gross thickness, maintaining their net thickness (corroded scantlings). The corrosion variation, $\delta_{Corrosion}$, over the service life of the ship accounting for a DMF is estimated as:

$$\delta_{Corrosion}\ =\ \frac{A_{net}}{A_{gross}} \tag{6.8}$$

where A_{gross} is the gross sectional area and A_{net} is the net sectional area.

The cost associated with the loss of cargo, C_C, in €, is estimated as (Garbatov et al, 2018):

$$C_c = C_{cargo} \times f_{cargo} \times P_{cargo} \tag{6.9}$$

where C_{cargo} = *1,200 €/ton* is the assumed value of the cost of a ton of cargo, f_{cargo} = 20% is the considered partial factor of the cargo lost and P_{cargo} is the total amount of cargo of the ship.

The total amount of cargo of the ship P_{cargo} is estimated according to the cargo configuration shown in *Figure 6.1*.

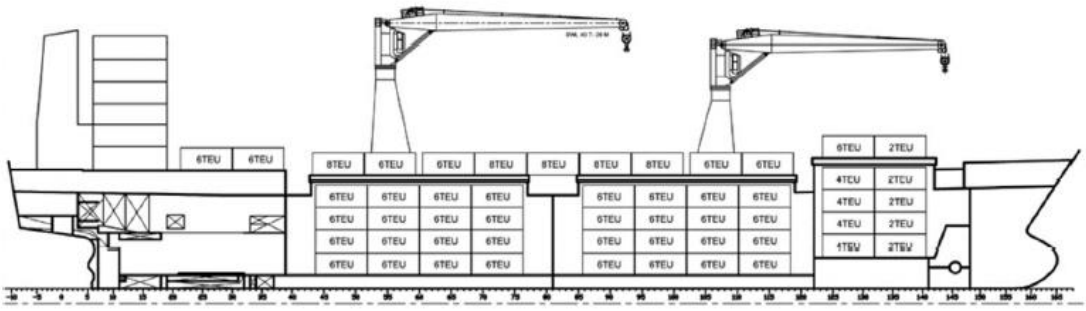

Figure 6.1 – Cargo configuration on multi-purpose ship (Garbatov et al, 2018).

In the present study, and to determine the maximum load, it was decided to consider that the containers are fully loaded, which is not the case in the realised situation.
Accounting for the number of 20-feet containers, the maximum cargo carried by the multi-purpose ship in this study is 300 TEU (Twenty-feet Equivalent Unit), that is, the total amount of cargo of the ship P_{cargo} = 7,200 ton. The dimensions and cargo capacity of 20-feet containers are shown in *Table 6.1*.

Table 6.1 – Dimensions and cargo capacity of 20-feet containers (Educargas Transitários, Lda).

Internal Dimensions	Door Dimensions	Maximum Volume	Cargo Capacity	Total Weight
Length(L) = 5.900m Width (W) = 2.350m Height(H) = 2.393m	Length(L) = 2.342m Height(H) = 2.280m	33.20m^3	21,770 Kg	24,000 Kg

The cost of the accident spill, C_d, in €, is estimated as:

$$C_d = f_{spill} \times P_{sl} \times CATS \times W_{fuel\ oil} \tag{6.10}$$

where f_{spill} = 10% is the considered partial factor of the fuel oil spill, P_{sl} = 10% is the probability that the fuel oil split reaches the shoreline (SØrgard et al.,1999), *CATS = 60 000 USD/ton* (SAFEDOR) or *53,595 €/ton* at the average exchange rate of 1€ to 1.12USD for the year 2019 (Banco de Portugal) is the cost of one ton accidentally spilt fuel oil and $W_{fuel\ oil}$ is the total weight of fuel oil in tonnes.

The total fuel oil capacity, $W_{fuel\ oil}$ onboard is estimated as (Parsons, 2003):

$$W_{fuel\ oil} = \frac{A}{V_s} \times P_w \times SFOC \times 10^{-6} \tag{6.11}$$

where *A* = 480h (20 days) is the assumed value of autonomy of the ship, V_s is the maximum service speed (see *Table 3.1*), in m/s, P_w is the effective propulsive power (see *Table 3.1*), in kW, *SFOC* = 170 g.kW/h is the assumed value of specific fuel oil consumption.

The costs associated with the loss of human life, C_v, in €, in this case, the loss of crew members is estimated as:

$$C_v = n_{crew} \times f_{crew} \times ICAF \tag{6.12}$$

where n_{crew} is the number of crew members (see *Table 3.1*), f_{crew} is the probability of loss of the life of a crew member (in this study, it is considered $f_{crew} = 25\ \%$ as used in a study performed by Horte et al., 2007), and *ICAF* is the implied cost of averting the fatality.

The implied cost of averting the fatality, *ICAF*, used in a study by Horte et al. (2007), can be estimated considering the statistics in OECD (2018).

$$ICAF = 7 \times \frac{GDP \times E}{4} \tag{6.13}$$

where *GDP = 46,180 USD/Capita* (*41,251 €/Capita* at the average exchange rate of 1€ to 1.12USD for the year 2019, Banco de Portugal) is the gross domestic product per capita and *E = 80.9 years* is the life expectancy at birth.

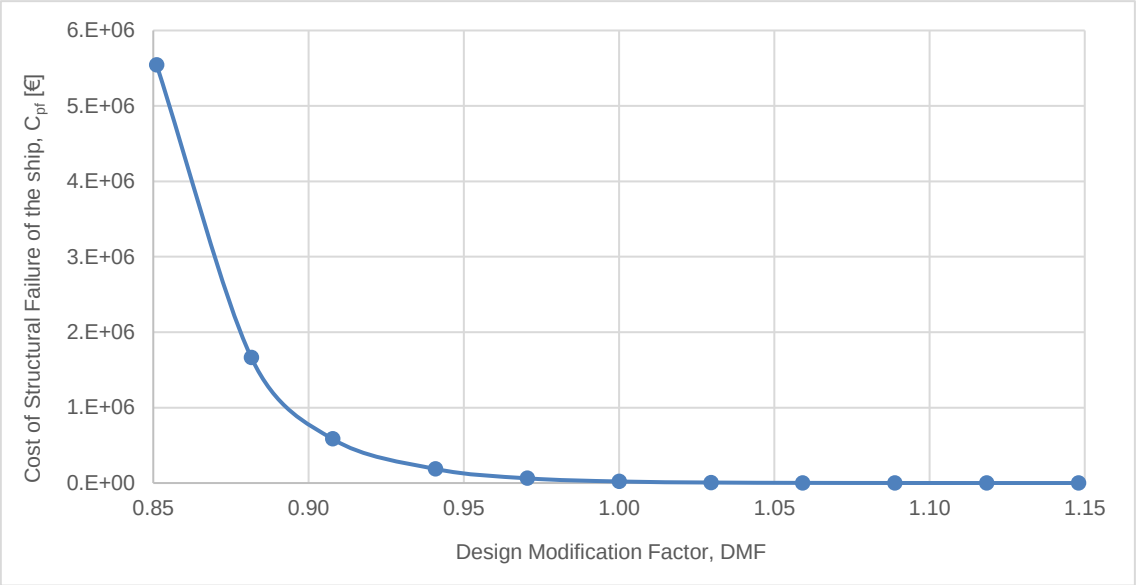

Figure 6.2 – Cost of structural failure of the ship, C_{pf} in €, for design modification factor (DMF).

6.2 Cost of implementing structural safety measures

The cost of implementing a structural safety measure accounts for the design modification factor (*DMF*), which is also associated with the reliability level (β), including the cost of material and labour, that is, the redesign of the midship section hull structure. The cost of structural redesign $C_{me}(DMF,\beta)$ is positive or negative depending on if the value of DMF is more significant or smaller than one respectively (Garbatov et al., 2018):

$$C_{me}(DMF,\beta) = \Delta W_{steel}(DMF,\beta) \times C_{steel} + C_{labour}(DMF,\beta) \tag{6.14}$$

where $\Delta W_{steel}(DMF,\beta)$ is the weight of steel, in tons, because of the design modifications factor (*DMF*), C_{steel} is the cost of steel ($k_A = 580\ €/ton$, see *Table 5.1*) and C_{labour} is the cost of labour of the constructing a $\Delta W_{steel}(DMF,\beta)$ defined by *CAPEX* estimate (C_{ma}, see *(5.54)*).

The weight of steel, in tons, because of the design modification factor (*DMF*) is estimated as (Garbatov et al, 2018):

$$\Delta W_{steel}\,(DMF,\beta) = (DMF-1) \times W_{steel} \tag{6.15}$$

where W_{steel} is the weight of steel related to the ship hull structural design estimated according to *CAPEX* (W_A, see *(5.49)*).

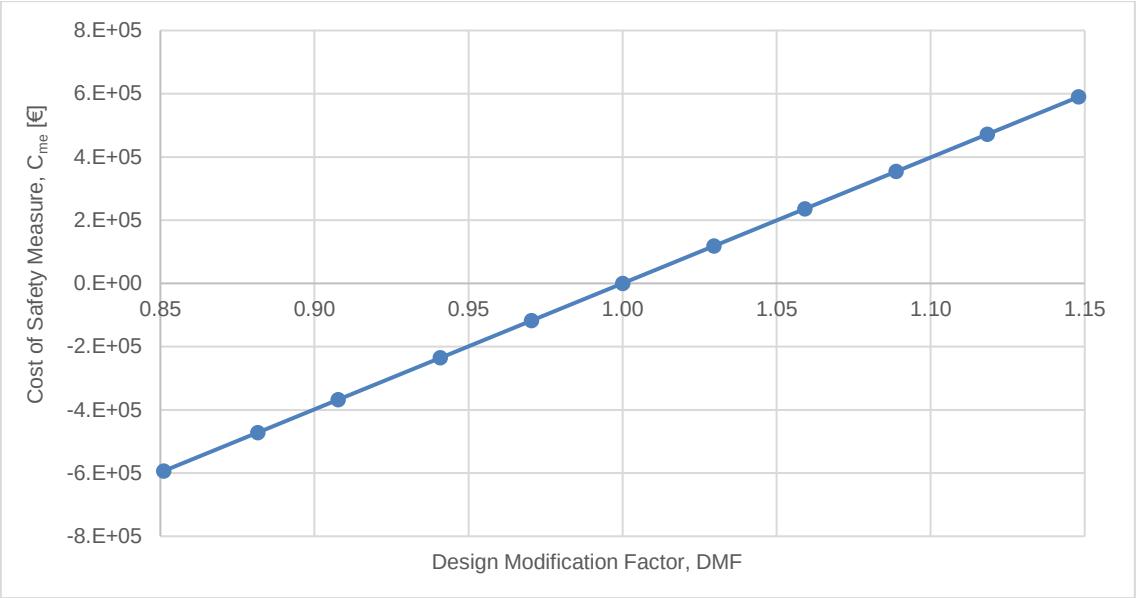

Figure 6.3 – Cost of safety measure, C_{me} in €, for design modification factor (DMF).

6.3 Optimum safety level

The main objective of the cost-benefit analysis is to identify an optimum level of ship safety, i.e., the optimum/target reliability index, controlling the risk associated with changing the initial design.

The cost-benefit analysis of the modified structure, according to the structural design modification factor (DMF) related to the scantlings of the midship section, varying the thickness of the main structural components, defined previously, is carried out based on the expected total cost (C_t), in €, defined as (Garbatov et al, 2018):

$$C_t = C_{failure} + C_{DMF} \tag{6.16}$$

where $C_{failure}$, in €, is the total cost associated with the progressive collapse of the ship's hull structure and C_{DMF}, in €, is the total cost of implementing structural safety as a function of the structural design modification factor (DMF), controlling the associated risk, involving the construction costs of the hull material (Steel), the quantity of material required and the labour cost as a function of the lightship weight.

Estimating the target reliability level β influences the structural failure cost associated with risk control since each of the costs defined above is a function of the reliability index β.

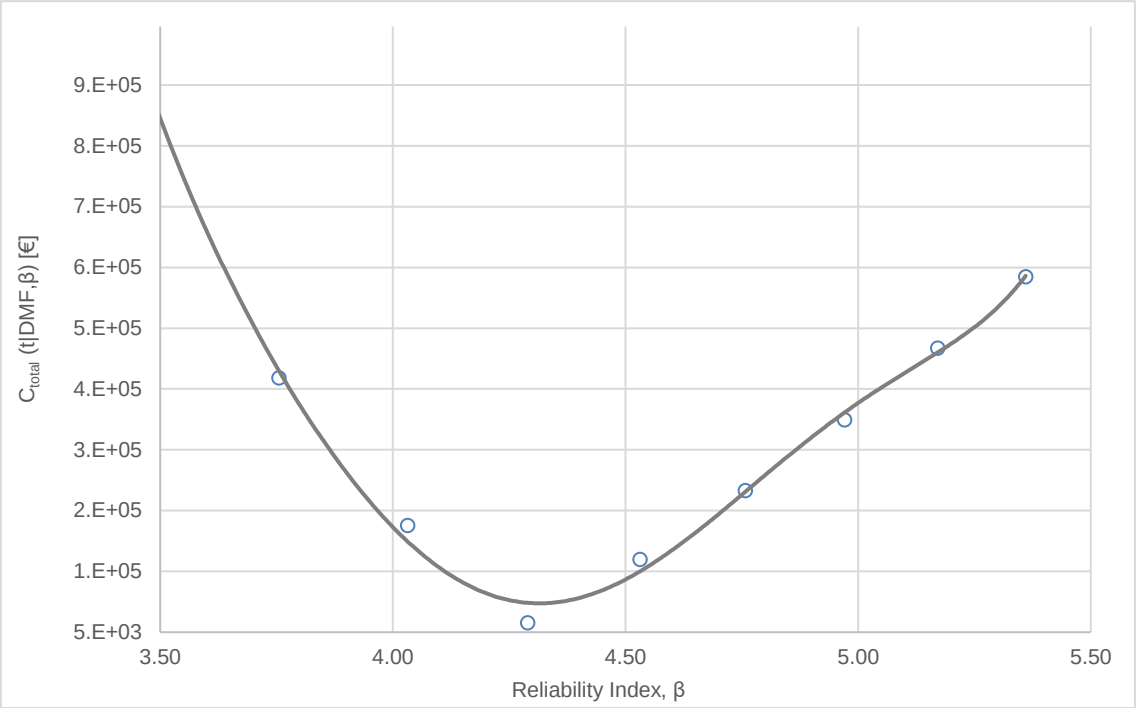

Figure 6.4 – Expected total cost, C_t, in €, as function for reliability index, β.

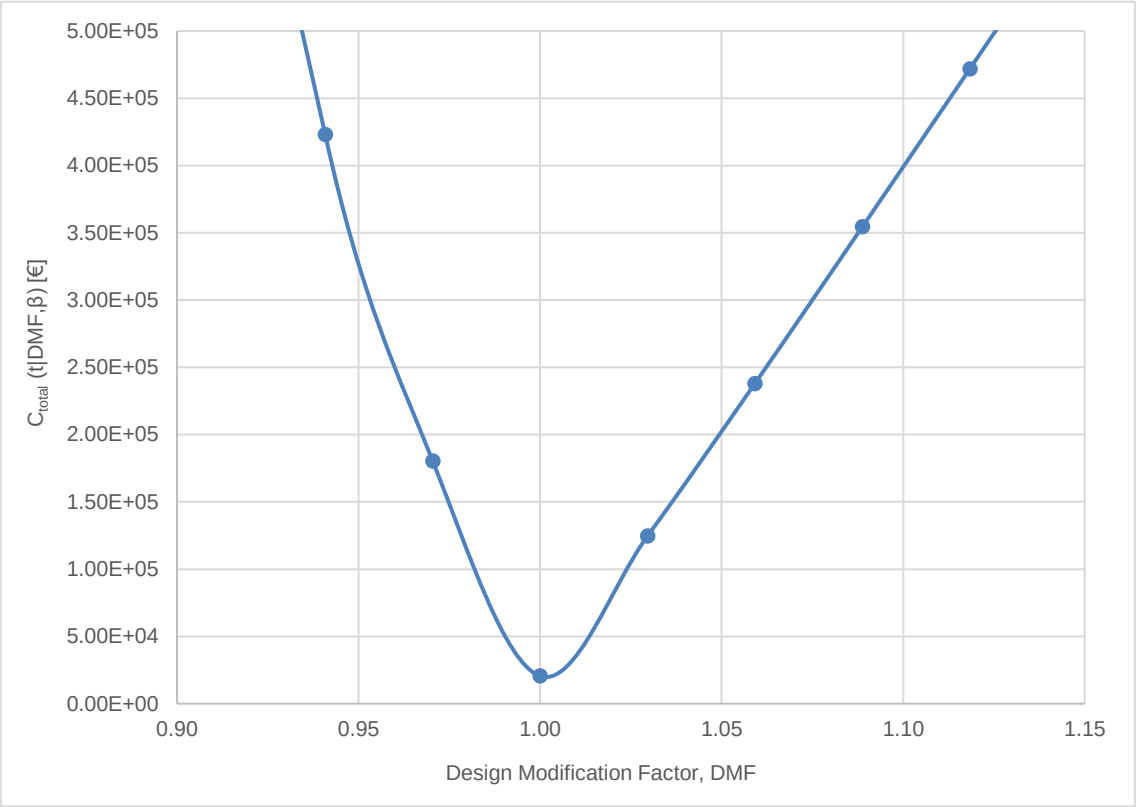

Figure 6.5 – Expected total cost, C_t, in €, as function for design modification factor, DMF.

The expected total cost (C_t) increase is increasing with decreasing failure probability concerning the progressive structural collapse (P_f), i.e., with increasing target reliability level (β) of the structure and therefore with increasing design modification factor (DMF).

During the service life (t_n = 25 years) of the ship's structural system, the reliability index (β) is estimated by minimising the risk associated with the probability of structural failure and the cost of the consequences, resulting in economic and human losses. According to the study, the range of values of the ideal/target reliability index (β) over the ship's service life can vary between 2.79 and 5.38.

The degradation of structural corrosion is reflected in the increased probability of failure as a function of the ship's life service.

Observing *Figure 6.4* and *Figure 6.5*, the selection of the ideal/target reliability level, which determines the probability of failure of the structural system and its consequences, corresponds to the minimum value of the curve of the expected total cost C_t (t|DMF, β), i.e., β = 4.33.

In selecting the optimum/target reliability level of the ship's structure, three methods are typically used (Garbatov et al., 2018):

a) Minimising the total risk associated with the probability of progressive failure of structural collapse, which results in economic and human losses in case of failed design.
b) Reasonable selection of the reliability level in the case of a new structural system with no previous history.
c) Calibration of the target reliability level according to the minimum requirements imposed by the classification societies in the choice of the plate panels and profiles to be used.

Garbatov & Sisci (2018) demonstrated that the partial safety factors related to the target reliability index (β) represent an acceptable risk level for the minimum cost in the structural design of a multipurpose ship. The three modification factors that impact the most on the reliability and cost of structural collapse are block coefficient, length and structural redesign.

6.4 External factors

The present study considers it an external factor in the increase/decrease in the price of raw materials. In this case, steel implies the risk analysis of the structure of a ship.

Due to armed conflicts, political and economic crises, natural disasters, climate change throughout human history, and the recent pandemic COVID-19, commodity price speculation is considerable, leading to fluctuating world market prices.

According to the base price of steel per tonne, K_A = 580 €/ton, a price increase of 20% and 50% was analysed, as well as a price decrease of the same order of magnitude.

It was assumed that the fluctuation in the price of steel K_A, in *€/ton*, would imply the resale or scrap price (C_{scrap} = 270 €/ton) of the ship, as they are related, i.e., it is increased or decreased in the same order of magnitude.

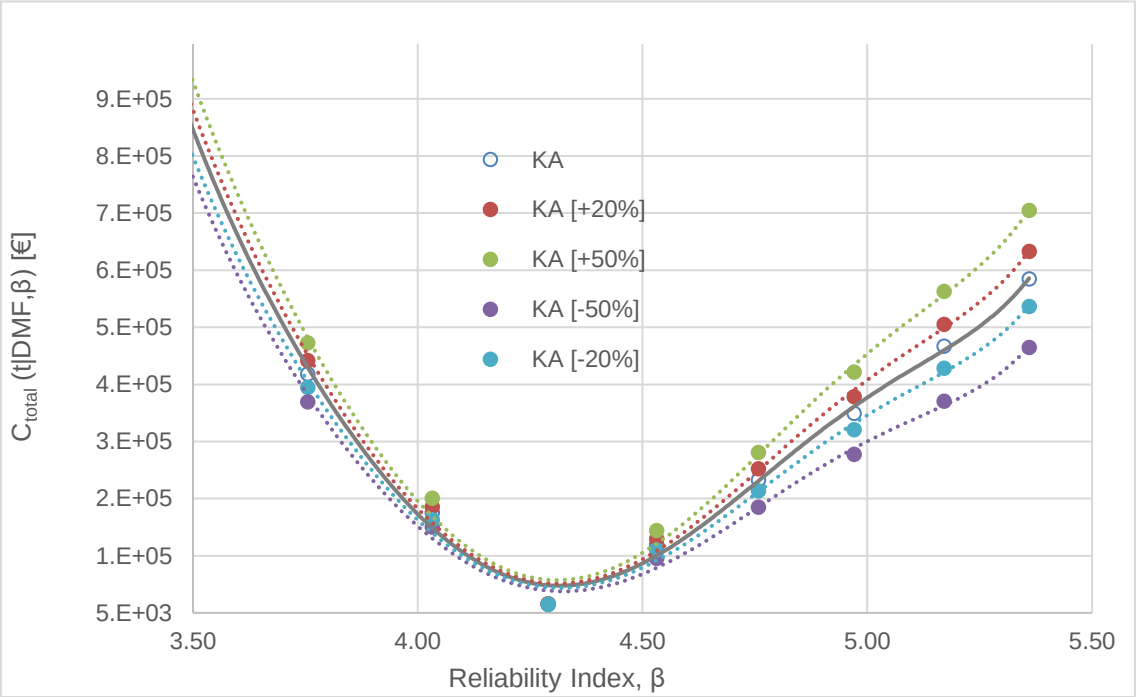

Figure 6.6 - Expected total cost, C_t, in €, as function for reliability index, β.

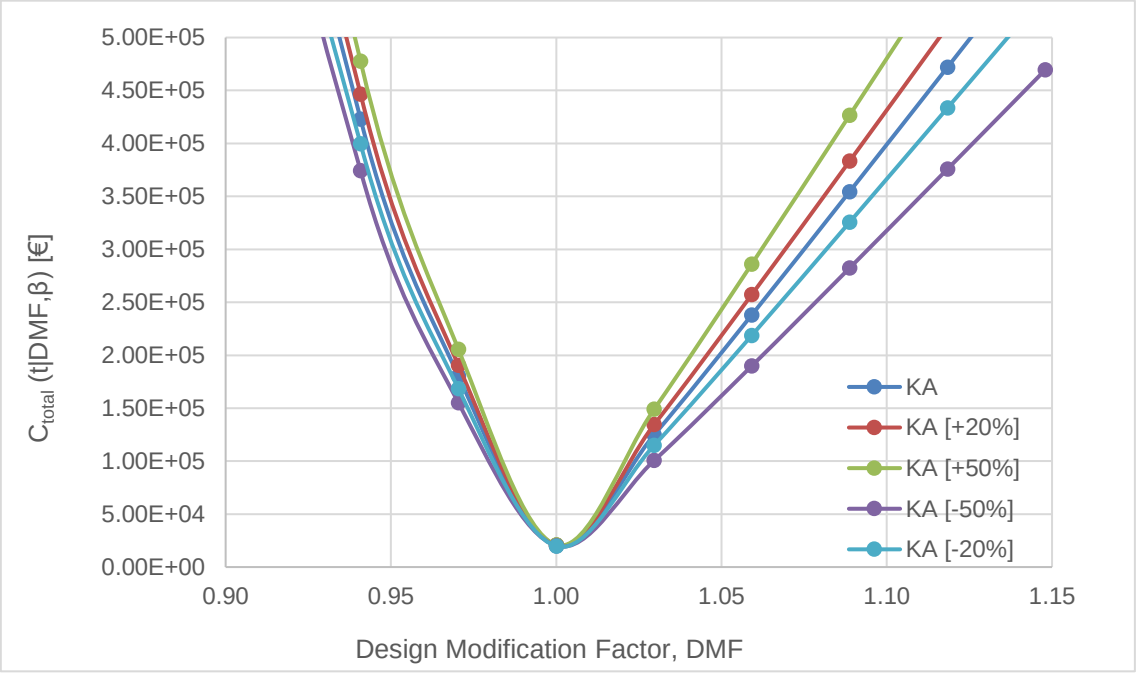

Figure 6.7 - Expected total cost, C_t, in €, as function for design modification factor, DMF.

Analysing the above graphs, *Figure 6.6* and *Figure 6.7*, we can observe that the base price of steel K_A = 580 €/ton, defined in the previous chapter, for a target reliability level β = 4.76, corresponding to a design modification factor DMF = 1.06, implies a total expected cost C_t = 237,934€. An eventual 50% increase in the steel price ($K_{A\ (+50\%)}$ = 870 €/ton) implies an increase in the total expected cost C_t = 286,021€. Comparing the two values, with a rise in steel price, the total cost increases by approximately 50,000€. A 50% depreciation in the price of steel ($K_{A\ (-50\%)}$ = 290€/ton), the total expected cost is C_t = 189,846€, a total cost saving of around 50,000€, i.e., the same value.

At a constant base steel price (K_A = 580€/ton), for different design modification factors (DMF), i.e., for different target reliability levels (β) of the structure, the total expected cost increases ($C_{t\ (DMF\ =\ 1.06)}$ = 237,934€; $C_{t\ (DMF\ =\ 1.09)}$ = 354,411€), i.e., the difference in total cost is approximate of the order of 120,000€. An increase in steel price increases the difference in total cost, i.e., for $K_{A\ (+50\%)}$ = 870 €/ton, the difference in expected total cost (C_t) rises to 140,000€. On the other hand, if there is a 50% depreciation in the price of steel ($K_{A\ (-50\%)}$ = 290€/ton), the difference in expected total cost (C_t) rises to 90,000€ but is based on lower-cost values.

7. CONCLUSION

Maritime transport represents about 90% of the existing commercial exchanges in the world. With the increase in competitiveness, the optimisation of more efficient structures, at a reasonable reliability level, for a lower construction cost, always complying with the minimum requirements imposed by the Classification Societies (CS), must be implemented in the structural design and construction of the ship, throughout its service life.

In the context of this work, a typical configuration of a cross-section of a multipurpose ship was dimensioned, whose type of cargo can vary (bulk, container, general cargo, refrigerated cargo...), subject to the different loads imposed by the Rules of the Classification Society Bureau Veritas (BV, 2019). The choice of the grade of material, the thickness of the plate panel and the profiles to be used in the structural definition of the midship section, according to the minimum requirements imposed by the Classification Societies, do not consider the economic aspects.

The cross-section risk analysis study is carried out using the first-order reliability method (FORM) and cost structure based on five newly built multipurpose ships to reduce the progressive structural collapse over the ship's service life (t_n = 25 years) at various target reliability indices, varying the design modification factor (DMF). The risk is associated with structural failure of the ship, cargo loss, accidental oil spill, loss of life and total loss of the ship.

The main objective of the cost-benefit analysis is to identify an optimum level of ship safety, i.e., the optimum/target reliability index, controlling the risk associated with the modification factor related to the resizing of the midship section structure by varying the thickness of the main structural components, based on the expected total cost.

The minimum value of the expected total cost risk curve is the optimised structural design solution that is most cost-effective, leading to lower construction and operational costs, satisfying existing requirements for safe transport, corresponding to the optimal/target reliability level of the structure that determines the probability of system failure and its consequences.

The methods implemented in the study are based on the limited data available during the initial design phase of the project and are considered approximate.

Several external factors have implications in the analysis of the cost of the ship, one of them being the fluctuation of the price of raw materials, in this case, steel. It is expected that the higher the design modification factor (DMF), that is, the higher the weight of steel, corresponding to a higher level of reliability of the structure, that is, a reduction in the progressive collapse of the structure, the impact of steel price fluctuation is more significant.

The choice of the target/ideal reliability level of the structure to be designed versus the design modification factor (DMF) should be as optimal as possible, as the impact of raw material fluctuation can increase costs.

8. REFERENCES

Amdahl, J., (2009), TMR4205 “Buckling and Ultimate Strength of Marine Structures”, Chapter 3: Buckling of Stiffened Plates.

Banco de Portugal – Eurosystem Statistics Exchange Rate year of 2019, [Online]. Available: https://www.bportugal.pt/en/taxas-cambio-lista.

Benford, H., (1967), “The Practical Application of Economics to Merchant Ship Design”, Marine Technology and The Society of Naval Architects and Marine Engineers (SNAME), 4 (01), pp. 519-536.

Bureau Veritas (BV, 2019), NR467 Rules for the Classification of Steel Ships, July 2019 edition.

Caprace, J.D., (2010), “Cost-effectiveness and complexity assessment in ship design within concurrent engineering and design for x framework”, Liège.

Cho, K., Arai, M., Basu, R., Besse, P., Birmingham, R., Bohlmann, B., Boonstra, H., Chen, Y., Hampshire, J., Hung, C., Leira, B., Moore, W., Yegorov, G., & Zanic, V., (2006), “Design Principles and Criteria”, Proceedings of 15th International Ship and Offshore Structures Congress (ISSC), pp. 521-599.

Cornell, C.A., (1969), “A probability-based structural code”, Journal of American Concrete Institute, No. 12, Vol. 66, pp.974–985.

Cudina, P., Zanic, V., & Preberg, P., (2010), “Multiattribute Decision Making Methodology in the Concept Design of Tankers and Bulk-Carriers”, Proceedings of the 11th Symposium on Practical Design of Ships and Other Floating Structures (PRADS), Rio de Janeiro, pp. 834-844.

Damyanliev, T., (2001), “Mathematical modelling at the valuation of the ship properties”, Proceedings of 3rd International Conference on Marine Industry (MARIND), Varna, Proc. Volume 3.

Damyanliev, T., (2002), “Program environment for Decision-Making Support Systems”, Proceedings of 1st International Congress MEET/MARIND, Varna, Proc. Volume 5, pp. 23-28.

Damyanliev, T., Georgiev, P., & Garbatov, Y. (2017), “Conceptual ship design framework for designing new commercial ships”, In: Guedes Soares, C. & Garbatov, Y. (eds.) “Progress in the Analysis and Design of Marine Structures”, London: Taylor & Francis Group, pp. 183-191.

Da-wei, G., & Gui-jie, S., (2018), “Reliability of hull girder ultimate strength of steel ships”, IOP Conference Series: Material Science and Engineering 317012036.

Ditlevsen, O.D., (1973), “Structural reliability and the invariance problem”, Research Report No. 22, Solid Mechanics Division, University of Waterloo.

Eurostat 2018 Estimated hourly labour costs for the whole economy in euros, [Online]. Available: http://ec.europa.eu/eurostat/statistics-explained/index.php/ Hourly_labour_costs.

Evans H. J., (1959), “Basic Design Concepts”, Journal of the American Society for Naval Engineers (ASNE), Vol. 71, pp. 671-678.

Evans, J., & Khoushy, D., (1963), “Optimized design of midship section structure”, Transactions of the Society of Naval Architects and Marine Engineers (SNAME), Vol. 71, pp. 144–191.

Freudenthal, A.M., Garrelts, M. & Shinozuka, M., (1966), “The analysis of structural safety”, Journal of the Structural Division, ASCE, 92, pp.267-326.

Garbatov, Y., Guedes Soares, C., & Wang, G., (2007), “Nonlinear time-dependent corrosion wastage of deck plates of ballast and cargo tanks of tankers”, ASME J. Offshore Mech. Arct. Eng., 129(1), pp.48-55.

Garbatov, Y., & Georgiev, P., (2017), “Optimal Design of Stiffened Plate Subjected to Combined Stochastic Loads”, In: Guedes Soares C. & Garbatov Y. (eds.) “Progress in the Analysis and Design of Marine Structures”, London: Taylor & Francis Group, pp. 243-252.

Garbatov, Y., Ventura, M., Guedes Soares, C., Georgiev, P., Koch, T., & Atanasova, I., (2017), “Framework for Conceptual Ship Design accounting for risk-based Life Cycle Assessment”, In: Guedes Soares, C., Teixeira, A. (Eds.), “Maritime Transportation and Harvesting of Sea Resources”, Taylor & Francis Group, London, pp. 921–931.

Garbatov, Y., Sisci, F., & Ventura, M., (2018), “Risk-based framework for ship and structural design accounting maintenance planning”, Ocean Engineering, 166, pp. 12-25.

Garbatov, Y., & Sisci, F., (2018), “Sensitivity analysis of risk-based conceptual ship design”. In: Guedes Soares, C., Santos, T.A. (Eds.), Progress in Marine Technology and Engineering, Taylor & Francis Group, London, pp. 499-510.

Guedes Soares, C., & Moan, T., (1988), “Statistical analysis of still-water load effects in ship structures”, Trans. Soc. Nav. Archit. Mar. Eng. (SNAME), 96, pp. 129–156.

Guedes Soares, C., (1990), “Stochastic modelling of maximum still-water load effects in ship structures”, ASME J.Ship Res., 34, pp. 199–205.

Guedes Soares, C., Dogliani, M., Ostergaard, C., Parmentier, G., & Pedersen, P.T., (1996), “Reliability-based ship structural design”, Trans. Soc. Nav. Archit. Mar. Eng. (SNAME), 104, pp. 359–389.

Guedes Soares, C., & Garbatov, Y., (1999), “Reliability of maintained corrosion protected plates subjected to non-linear corrosion and compressive loads”, Mar. Struct., 12 (6), pp. 425–445.

Guia, J., Teixeira, A.P., & Guedes Soares, C., (2018), “ Probabilistic modelling of the hull girder target safety level of tankers”, Marine Structures, 61, pp. 119-141.

Harlander, L., (1960), “Optimum plate-stiffener arrangement for various types of loading”, J. Ship Research, 20/4, pp. 49–65.

Hasofer, A.M., & Lind, N.C., (1974), “An Exact and Invariant First Order Reliability Format”, Journal of Engineering Mechanics Division, ASCE, Vol. 100, pp. 111-121.

Horte, T., Wang, W., & White, N., (2007), “Calibration of the hull girder ultimate capacity criterion for double-hull tankers”, In: Proceedings of the 10th International Symposium on Practical Design of Ships and Other Floating Structures (PRADS), Houston, USA, pp. 235–246.

Hughes, O., Mistree, F., & Zanic, V., (1980), “A practical method for the rational design of ship structures”, J. Ship Research, 24(2), pp. 101–113.

Hughes, O., (1988), “Ship Structural Design: A Rationally-Based, Computer-Aided Optimization Approach”, In Wiley-Interscience.

Khajehpour, S., & Grierson, D. (2003), “Profitability versus safety of highrise office buildings”, Structural Multidisciplinary Optimization, 25, pp. 279–293.

Klanac, A., & Kujala, P., (2004), “Optimal design of steel sandwich panel applications in ships”, In: Proceedings of the PRADS, pp. 907-914.

Melchers, R.E., (1999), “Structural reliability analysis and prediction second”, (Eds.) John Wiley and Sons, ed., Chichester, West Sussex, England.

Nowacki, H., Brusis, F., & Swift, P., (1970), “Tanker preliminary design - An optimization problem with constraints”, Trans. SNAME, 78, pp. 357–390.

OECD (Organisation for Economic Co-operation and Development) Data year of 2018, [Online]. Available: https://data.oecd.org.

Paik, J.K., & Thayamballi, A.K., (2008), “Ultimate Limit State Design of Ship Hulls”, The Society of Naval Architects and Marine Engineers (SNAME) vol.110.

Parsons, M.G., (2003), “Parametric design”, Chapter 11 of “Ship Design and Construction”, Vol. I, Lamb (Ed.).

Parsons, M. G., & Scott, R. L., (2004), “Formulation of multi-criterion design optimization problems for solution with scalar numerical optimization methods”, J. Ship Research, 48, pp.61–76.

Rigo, P., (2003), “An integrated software for scantling optimization and least production cost”, Ship Technology Research, Schiffahrts-Verslag, 50, pp. 126-141.

Rigo, P. & Caprace, J., (2011), “Optimization of ship structures”, Marine Technology and Engineering, 2.

Rogal, J.E., Tase, A., Lockett, R.D., & Koenig, P.C., (2016), “Analysing and Forecasting overhead costs in U.S. Naval Shipbuilding”.

Ross, J. & Hazen, G., (2002), “Forging a real-time link between initial ship design and estimated costs”, ICCAS, pp.75-88.

Seo, S., Son, K., & Park, M., (2003), “Optimum structural design of naval vessels”, Marine Technology, 40/3, pp. 149–157.

Skjong, R., Vanem, E. and Endersen, Ø., (2005), “Risk evaluation criteria”, SAFEDOR report D452, [Online] Available: www.safedor.org/resources/index.html.

Smith, C., (1977), “Influence of local compressive failure on ultimate longitudinal strength of a ship's hull”, Proceedings of the International Symposium on Practical Design in Shipbuilding, pp. 73-79.

Sørgard, E., Lehmann, M., Kristoffersen, M., Driver, W., Lyridis, D., & Anaxgorou, P., (1999), “Data on consequences following ship accidents”, Safety of shipping in coastal waters (SAFECO II), DNV, WP III.3, D22b.

Steelbenchmarker, (2019). Dollars per metric tonne steel, [Online]. Available: www.steelbenchmarker.com.

United States Maritime Administration (MARAD), (2018). Guideline Specifications for Merchant Ship Construction [Online]. Available: https://www.marad.dot.gov/.

Xuebin, L., (2009), “Multiobjective optimization and multiattribute decision-making study of ship’s principal parameters in conceptual design”, J. Ship Research, 53, pp. 83–92.

Yeter, B., Garbatov, Y., & Guedes Soares, C., (2016a), “Modular jacket offshore wind turbine support structure for the Northern Portuguese coastal zone”, In: Guedes Soares, C.(ed.) Progress in Renewable Energies Offshore. London, UK: Taylor & Francis Group, pp. 655-663.

Yeter, B., Garbatov, Y., & Guedes Soares, C., (2016b), “Structural design of an adaptable jacket offshore wind turbine support structure for deeper waters”, In: Guedes Soares, C. & Santos, T. (eds.) Maritime Technology and Engineering. London: Taylor & Francis Group, pp. 583-594.

Yeter, B., Garbatov, Y., & Guedes Soares, C., (2017), “Risk-based multi-objective optimisation of a monopile offshore wind turbine support structure”, Proceedings of the 36th International Conference on Ocean, Offshore and Arctic Engineering, OMAE17, Trondheim, Norway. paper OMAE2017-61756.

Zanic, V., Andric, J., & Prebeg, P., (2005), “Superstructure deck effectiveness of the generic ship types - A concept design methodology”, IMAM, pp. 579-588.